UNIVERSITY OF SOUTHAMPTON

Faculty of Physical Science and Engineering

Department of Electronics and Computer Science

Master of Philosophy Thesis

Supervisor: Dr Harold M.H. Chong

AN INVESTIGATION INTO A CATALYST FREE PECVD NANOCRYSTALLINE GRAPHENE/GRAPHITE ON INSULATOR

Zainidi Haji Abdul Hamid

4th October 2017

UNIVERSITY OF SOUTHAMPTON

ABSTRACT

Faculty of Physical Science and Engineering

Department of Electronics and Computer Science

An Investigation of a Catalyst Free PECVD Nanocrystalline Graphene / Graphite on Insulator

By Zainidi Haji Abdul Hamid

The unique electrical and optical properties of graphene have attracted application as transparent electrodes, transistors and photodetectors. However, the small flake size of mechanical exfoliated graphene has limited its scalability to large area production. Recently, large area graphene is produced through chemical vapour deposition (CVD) and epitaxial growth method. CVD of graphene on insulator or metal-catalyst is considered low cost and process flexible. This is because graphene film quality and deposition rate can be controlled through process parameters such as temperature, gas flow rate and gas mixture. Large area CVD graphene on metal-catalyst such as Ni or Cu is amongst other established method but the need for processing steps, such as film transfer and metal etching can ultimately damage the graphene and affect device performance. Therefore, the research attention is now focused on catalyst free CVD graphene process on insulator materials such as silicon dioxide (SiO_2).

In this work, the nanocystalline graphene/graphite (NCG) films are synthesised in a mixture of methane (CH_4) and hydrogen (H_2) environment using radio frequency chemical vapour deposition (RF PECVD) without metal transition catalyst, deposited directly onto 150 mm diameter silicon wafer with an insulating substrate, such as SiO_2, is presented. The as-deposited NCG films properties depend on deposition conditions such as growth temperature, growth time, pressure, mixtures or flow rates of precursor, RF power and substrate material. Initially, the growth temperatures are varied in the range of 600 °C to 850 °C, while keeping other deposition parameters unchanged, and subsequently the properties of the as-deposited NCG film is studied. The nanocrystalline nature of as-deposited film are analysed based on their Raman spectra, whereas the film thickness and sheet resistances are characterised using ellipsometry spectroscopy and a simple four point probe measurements respectively.

The electrical properties of the NCG films are performed using I-V measurement on a simple two terminal device with titanium/nickel (Ni/Ti) contacts. Transmission line method (TLM) structures with Ni/Ti probe pads are also fabricated for contact and sheet resistances measurement purposes.

CONTENTS

List of Figures

List of Tables

DECLARATION OF AUTHORSHIP

I, **Zainidi Haji Abdul Hamid** declare that this thesis and the work presented in it are my own and has been generated by me as the result of my own original research.

AN INVESTIGATION OF A CATALYST FREE PECVD NANOCRYSTALLINE GRAPHENE / GRAPHITE ON INSULATOR

I confirm that:

1. This work was done wholly or mainly while in candidature for a research degree at this University;

2. Where any part of this thesis has previously been submitted for a degree or any other qualification at this University or any other institution, this has been clearly stated;

3. Where I have consulted the published work of others, this is always clearly attributed;

4. Where I have quoted from the work of others, the source is always given. With the exception of such quotations, this thesis is entirely my own work;

5. I have acknowledged all main sources of help;

6. Where the thesis is based on work done by myself jointly with others, I have made clear exactly what was done by others and what I have contributed myself;

7. Either none of this work has been published before submission, or parts of this work have been published at international conference proceedings (Page 3).

Signed : ……

Date : 4th October 2017

ACKNOWLEDGEMENTS

First and for most, the author would like to convey his sincere gratitude and many thanks to his supervisor, Dr Harold M H Chong, for giving him the opportunity to join his group and continuous advice, guidance, suggestions and encouragement throughout the course of his research endeavour.

He also would like to express his appreciation and thanks to his colleague, Sam Fishlock, for his help, assistance and friendship throughout the work. The author also would like to acknowledge the support of the Government of Brunei in-service training scheme through the Institut Teknologi Brunei for giving him the opportunity to pursue his PhD undertaking. Many thanks also go to Southampton Nanofabrication Centre and Oxford Instrument for the support of the project.

A special gratitude and appreciation to the author's wife, Zarinah Mohammad, who always been around and giving a constant source of inspiration throughout the research work. Finally, he wishes to express his gratitude and thanks to his family and parents for their continuous morale support, encouragement and understanding throughout the journey of his study.

CHAPTER 1

Introduction

1.1 Definition of the problem and Motivations

Graphene - one of the carbon allotropes which is planar, two-dimensional one atom thick layer arranged in a hexagonal structure. It is a zero gap semiconductor or zero–overlap semimetal [1] with linear energy dispersion relation near the dirac points where the conduction and valence touch. It is a promising materials for many applications especially graphene based electronic devices, mainly due to its unique electronics properties [1] such as high carrier mobility, quantum hall effect at room temperature, ballistic transport, which have led the major driving force in research areas.

Other graphene properties such as mechanically flexible, high optical transmittance, has also indulge itself as a good candidate for a replacement, if not to complement silicon technology as used in electronic devices such as FET, solar cells, gas and chemical sensors. Among many possible applications, graphene has been studied in the fields of *transparent conductive electrodes* due to its potential to fulfil the requirements of various devices such as touch screens, optical devices, thin film transistor (TFT), and solar cell. As reported in [2], several issues on thin film technology pertaining to transparent conductive film such as improvement of electrical conductivity, enhancement of mechanical flexibility and materials cost reduction have been highlighted. At present indium tin oxide (ITO) has been widely used in many applications due to its low sheet resistance [2] (10-25 Ω/square with above 90% transmittance). However, ITO films are unlikely to fulfil future needs due to losses in conductivity on bending and high cost due to its scarcity. Recent advances in the synthesis and characterization of graphene suggest that it may be suitable for many electronic applications including as a transparent conducting electrodes for solar cells, where large area, continuous graphene is required.

There are several methods of synthesizing graphene. Mechanical exfoliation [3, 4] is widely used for fundamental studies but it is not suitable for mass production due to its low yield, randomly scattered on the substrate and time consuming.

Thermal decomposition of silicon carbide (SiC) [5-7] enables large area synthesis of graphene. Although this technique is simple and high quality monolayer graphene can be produced but it requires high thermal process temperature (up to 1650 °C) and ultrahigh vacuum (UHV), difficult to exfoliate the grown graphene to desired substrate due to the strong cohesive strength of the graphene/SiC interface and extreme chemical stability of SiC makes it less attractive.

Chemical vapour deposition (CVD) on various transition metals or foils [8-11] is another technique which is superior to others from the technological applications perspective due to its capability in producing high quality mono, bi- and few-layers graphene in large scale. This method of deposition helps to decompose hydrocarbon gases and promote the nucleation of graphene. It is compatible with current semiconductor manufacturing process and cost effective towards direct integration of produced graphene with existing silicon technology. However, this method requires the as-deposited film to be transferred to a desired insulating functional substrate such as SiO_2, by using chemical etching methods. These processes even though are possible but it is time consuming, complex and may degrade the electronics transport properties of the already good quality produced graphene film, may contaminated with the transition metal and/or with chemical residue, wrinkles, pin holes and cracks. In addition to that, high thermal budget is also required as most CVD process on transition metal requires high temperatures in the range of 900°C to 1100 °C and this would likely damage other devices being prepared on low melting temperature substrates.

Hence, in order to avoid these drawbacks many research groups [12-17] based on CVD processes have been developed to explore on the synthesis of graphene film directly onto substrates such as SiO_2, Si, Al_2O_3, Si_3N_4 etc. at low temperature which is far better for integration of graphene based materials with other electronics device applications. But the resultant film on insulating substrate is of low quality nanocrystalline graphene (NCG) [15] with defects in contrast with metal CVD method, and these still require further optimisation of deposition parameters to produce large size and high quality graphene. However, this approach is complex and challenging and even to date the mechanism or role of the non-metal catalyst in CVD still poorly understood. It is still at infant stage and require further work in order to improve critical issues such the quality, the control of number of layers of the film are still yet to be resolved before graphene based electronic devices can be commercialised.

The interesting part of these NCG film as synthesized on non-transition metal catalyst CVD is that, they are continuous, transparent and electrically conductive and has potential application in transparent conductive films. If the NCG film qualities can be further optimised, it would be beneficial and a better option over transferred graphene technique whereby breaking of the film during transfer step and trapping impurities at the interface amongst other possibilities can be minimised.

Hence, the motivation of this project is to synthesize large area nanocrstalline/microcrystalline graphene (NCG/µCG) film in a reproducible manner, directly onto an insulator substrate without metal catalyst at deposition temperature from 600 °C to 850 °C and the film is aimed as transparent conducting layer application.

This research reports on the novel deposition technique, fabrication and characterisation of nano/microcrystalline graphene films (NCG), deposited directly on SiO_2 by using radio frequency plasma enhanced chemical vapour deposition technique (RF-PECVD). This technique not only allows

deposition on wafer scale size but also at low deposition temperature (as low as 650 °C) as compared with thermal CVD, with the use of plasma, as well as compatible with the current silicon technology.

1.2 Objectives

The main aim of this research is to explore the synthesis of NCG film using RF PECVD directly on insulating substrate, such as SiO_2 without transition metal catalyst. This involves developing a process for the synthesis of NCG films, which are electrically conductive and optically transparent in the range of visible and infrared region, deposited at low deposition temperature as possible. In order to achieve this, obviously several deposition conditions or parameters such as growth temperature, growth time, pressure, mixtures or flow rates of gases, and RF power need to be experimentally conducted and tuned. Subsequently, the as-deposited NCG film, electrical properties are then characterised and analysed.

The following are the specific objectives of this work:

- To study the effect of varying growth deposition temperature (between 600 °C - 850 °C) on the as-deposited film.
- To characterise the as-deposited film properties in terms of their Raman spectra, sheet resistance, deposition rate, grain size and optical transparency.
- To fabricate test structures and devices based on the as-deposited film.
- To electrically characterise the fabricated structures based on the as-deposited film.
- To investigate on how to optimise the as-deposited NCG in terms of their electrical properties.

1.3 Novel Contribution

- Successfully developed a process whereby reproducible synthesis of NCG film directly on an insulator, for example SiO_2 and silicon, without transition metal catalyst using RF-PECVD has been achieved.
- Low growth deposition temperature of 650 °C has been achieved to synthesize the NCG film.

1.4 Conference Proceedings

- Graphene 2013 in ImagineNano 2013 Conference held from 23-26 of April, 2013 in Bilbao Spain (Poster presentation).
- 39th International Conference on Micro and Nano Engineering (MNE), London 16-19 Sept 13 (Poster presentation).

1.5 Report Outline

- **Chapter 2** presents a literature review related to graphene. This includes carbon and its allotropes, what graphene is and some of its properties, different methods of synthesizing graphene, and growth of NCG film directly on insulators without catalyst, and transparent conductor application and criteria.

- **Chapter 3** describes basic principle of PECVD.

- **Chapter 4** deals with the synthesis of the NCG film, characterisation of the as-deposit films.

- **Chapter 5** details the test structure fabrication processes and electrical characterisation.

- **Chapter 6** Conclusion and future works.

CHAPTER 2
Literature Review

2.1 BACKGROUND

2.1.1 Carbon and Its Allotropes

Carbon (symbol C), is the six element on the periodic table. It is one of the most abundant element in the Earth's crust, and the fourth most abundant element in the universe by mass after hydrogen, helium and oxygen. Carbon is the fundamental building block of all living organism, thus all carbon containing compounds are known as organic compounds.

Elemental carbon exists in two natural allotropes that is, diamond and graphite. Basically, carbon allotropes differ in the way the atoms bond with each other and array themselves into a structure resulting each have different physical and chemical properties.

In this report, some allotropes of carbon are discussed briefly as follows:

Graphite

The structural diagram of graphite is as shown Figure 3. In graphite, the carbon atoms form planar, or flat, layers. Each layer is made up of rings containing six carbon atoms forming a series of continuous hexagon structures. Each atom has three sigma (σ) bonds and belongs to three neighbouring rings. The fourth electron of each atom becomes part of an extensive pi (π) bond system. The free movement of π bonds (delocalised electron) throughout the molecule enable graphite to conduct electricity. Bonds (σ bond) between atoms within a layer of graphite are strong, but the interlayer bonds (π bond) are weak and easily slide giving rise to one of graphite's physical properties, that is softness. The graphite layers can easily be removed and makes it as a good lubricant.

Diamond

The diamond structure is shown in Figure 1a. Diamond is the most stable form of pure carbon - formed under high temperatures and pressure under earth's crust. Each atom in a diamond is bonded tetrahedrally to four other carbon atoms to form a three-dimensional lattice. The shared electron pairs are held tightly in σ bonds between adjacent atoms leaving no free electron. Diamond is rather inert and reacts with few chemicals due to its compact crystal lattice. They are good thermal conductors and electrical insulators.

Amorphous carbon

Amorphous carbon refers to carbon that does not have a crystalline structure (Figure 1g). Some examples of amorphous carbons are charcoal and soot. The properties of amorphous carbon depend on the ratio of sp^2 to sp^3 hybridized bonds present in the material; high in sp^3 hybridized bonds are referred to as tetrahedral amorphous or diamond-like carbon.

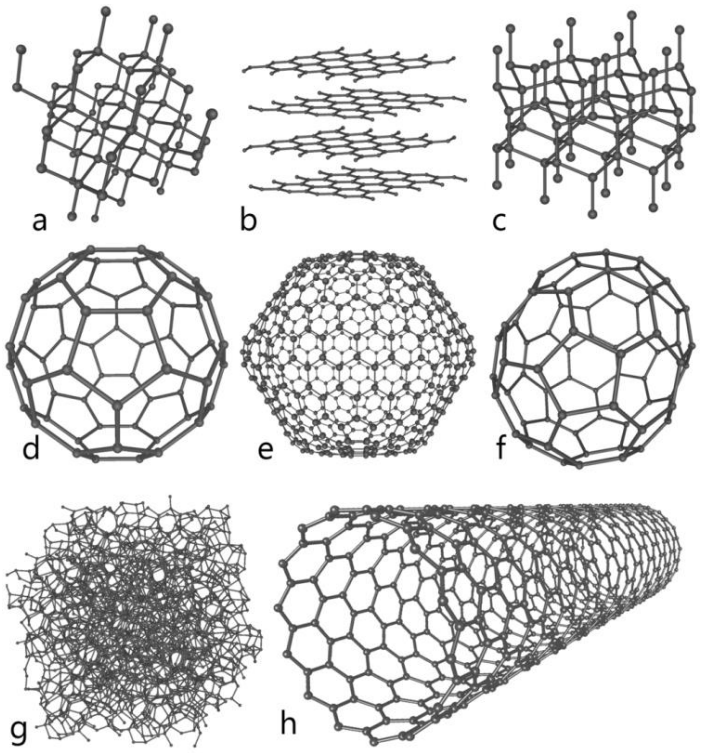

Figure 1. Allotropes of carbon: (a) Diamond, (b) Graphite, (c) Lonsdaleite, d) C60 (Buckminsterfullerene or buckyball), (e) C540, (f) C70, (g) Amorphous carbon, and (h) single-walled carbon nanotube, or buckytube. Reproduced from [18].

Fullerenes

Fullerenes are another form of carbon allotropes. Basically, fullerenes are molecules of varying sizes composed entirely of carbon that take on the form of hollow spheres, ellipsoids, tubes, and many other shapes.

Buckminster Fullerene, (C_{60}) as shown in Figure 1(d), also known as fullerenes or buckyballs in short, were discovered in 1985 and named after an architect engineer, R. Buckminster Fuller. They have spherical molecules containing pentagonal and hexagonal rings with no two pentagons share an edge, and assembles similar to football ball having twenty hexagons and twelve pentagons, with a carbon atom at the vertices of each polygon.

Cylindrical or tube fullerenes are called nanotubes, having a few nanometres wide with length ranging from micrometres to several millimetres. They are very strong and good conductors of electricity, which makes them useful in reinforcing structures where exceptional lightness and strength are needed, for example the frame of a tennis racket, and as semiconductors in electronic circuits respectively. They have been the subject of intense research, due to their unique chemistry and applications in materials science, electronics, and nanotechnology.

2.2 What is Graphene?

Graphene is a single-atom thick planar sheet of graphite with sp^2 hybridized carbon atoms arranged in two dimensional (2D) honey comb crystal lattice. It is referred to the mother of all graphitic forms [1], that is, the basic building block of other important allotropes (different forms of the same element whereby the same atoms bond together in different ways) of carbon dimensionalities namely; three dimensional (3D) *graphite* if several single atom sheets are stacked together, one-dimensional (1D) *carbon nanotubes* if a single sheet rolled into and zero-dimensional (0D) *fullerenes* if wrapped up as illustrated in Figure 2.

The term graphene is only refers to a quasi-two dimensional isolated monolayer of carbon atom that are arranged in hexagonal lattice [4]. The carbon–carbon bond length in graphene is about 0.142 nm. Several graphene sheets stack to form graphite with an interplanar spacing approximately 0.34 nm. The hybridized sp^2 bonding of graphene as in **Figure 3** shows three in-plane sigma (σ) bonds per C atom, work as the rigid backbone of the hexagonal structure, and pi (π) orbitals perpendicular to the plane of the lattice, control interaction between different graphene layers and the supporting substrate which eventually influencing its electronic properties.

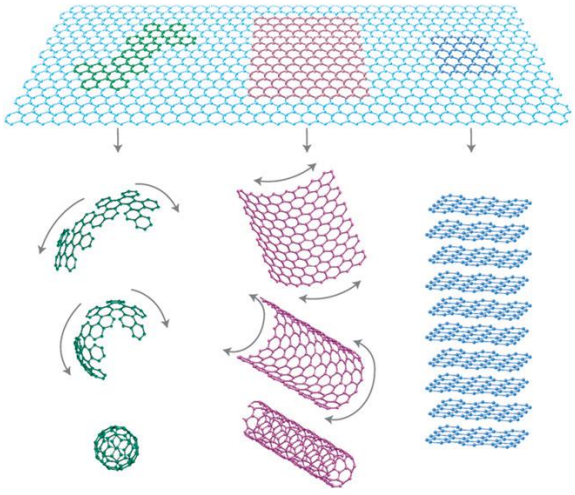

Figure 2. Different types of allotropes of carbon: 2D Graphene (top), 0D fullerene (left), 1D nanotube (middle) and 3D graphite (right). Reproduced from [1].

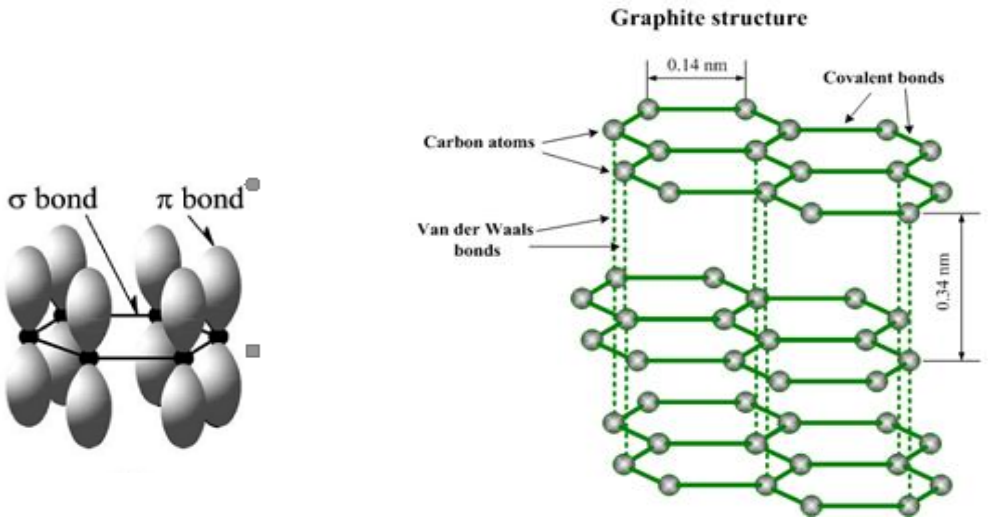

(a) (b)

Figure 3. Structure of graphite. (a) Schematic of the in-plane σ bonds and the π orbitals perpendicular to the plane of the sheets. Reprinted from [19] (b) Crystal lattice of graphite. (Reproduced from www.substech.com)

2.3 Properties of Graphene

In order for the applications of graphene can be well understood, the basic properties of graphene need to be studied first. In this section, the structures and some of the important and attractive properties of single (SLG), b (BLG) and few-layers (FLG) graphene are highlighted.

2.3.1 Structure of graphene

The electronic properties of graphene depend on the number of layers of graphene [1]. The different structures of graphene are as follows: a SLG is a single 2D hexagonal sheet of carbon atoms; BLG and FLG graphene has two and 3 to 10 layers of such 2D sheets respectively and, thick graphene sheet is referred to anything more than 10 layers.

2.3.2 Properties of Single, Bi-layers and Few layers graphene

SLG has a unique electronic structure whereby it shows band-overlap in two conical points (K and K') in the Brillouin zone [Figure 4(a)]. This is a typical of semi metal. In this structure, the charge carriers, also known as mass-less Dirac fermions, are electrons losing their rest mass, m_0. At room temperature, SLG shows ambipolar characteristics [Figure 4(b)], i.e., the charge carriers can be tuned between holes and electrons depending upon the nature of the gate voltage [20].

BLG shows a gapless state with parabolic bands touching at K and K', in contrast to conical bands of single-layer graphene. Hence, it is considered as a gapless or zero-gap semiconductor. Its charge carriers have finite mass or known as massive Dirac fermions.

Both SLG and BLG show very high transparency for light waves in the range of ultra-violet to infra-red that makes them suitable for transparent electrode [21] applications.

FLG which has 3-10 layers, the valence and conduction start to overlap. Any structure consisting more than 10 layers can be considered as a thin film graphite.

Generally, graphene is used to describe a single layer of the honeycomb carbon, however it is also used in the context of BLG, FLG and even multilayer graphene (MLG) as traditionally referred to graphite. In this work, the as-deposited film is referred to nanocrystalline graphene or graphite (NCG).

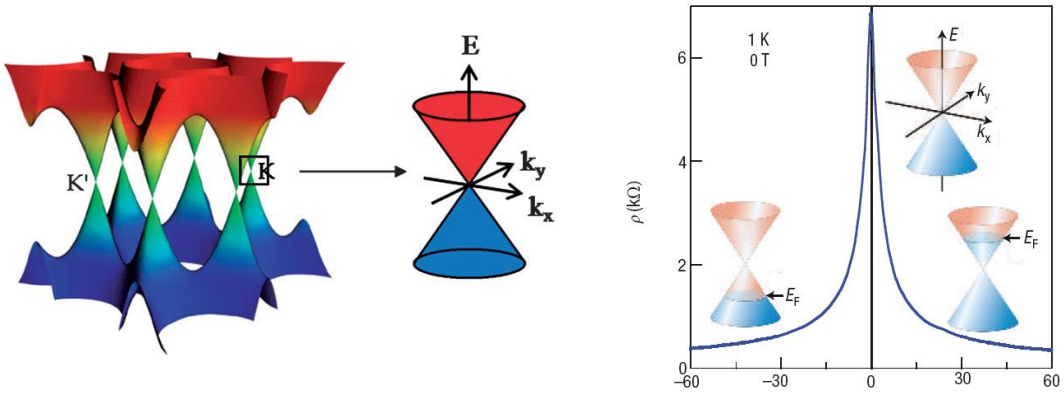

(a) (b)

Figure 4. (a) Electronic band structure of, and (b) Ambipolar electric field effect of single-layer graphene. The insets show the position of the Fermi energy, E_F with changing gate voltage V_g. Positive (negative) V_g induce electrons (holes) in concentrations. The rapid decrease in resistivity ρ on adding charge carriers indicates their high mobility. Reproduced from [22] and [1] respectively.

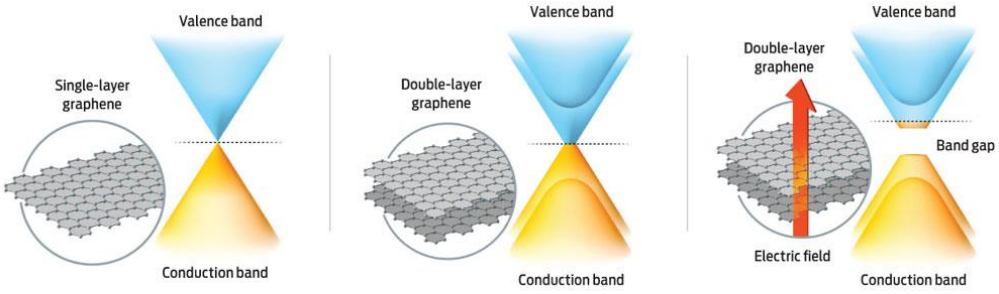

(a) (b) (c)

Figure 5. (a) and (b) show SLG and BLG valence and conduction bands meet at a K point, with no band gap. (c) When an electric field is applied perpendicular to the layers, a small band can be tuned to some extent. Reproduced from [23].

2.4 Methods of Obtaining Graphene

The synthesis of graphene can be broadly classified into two different approaches:

- Exfoliation methods - whereby graphene is derived from an existing graphite crystal (top-down approach), and
- By growth process of graphene film directly onto a substrate surface (bottom-up approach).

2.4.1 Exfoliation method

Graphite is layers of many graphene sheets stacked and bonded together by weak van der Waals force. Theoretically, if these weak bonds can be broken apart, it is possible to separate out individual graphene layer from a high purity graphite sheets. This can be done mechanically or chemically. Here, only a mechanical exfoliation technique is briefly mentioned.

2.4.1.1 Mechanical exfoliation

This simple technique of preparing graphene was demonstrated by a Nobel prize in Physics awardees, Prof. Andre Geim and Prof. Konstantin Novoselov, University of Manchester, where they used an adhesive tape [3] to detach graphene from a graphite crystal. Multiple layers of graphene still remains on the tape after peeling it from bulk graphite and by repeated peeling process, it cleaved into various flakes of few layer graphene. Then the tape is attached to a substrate and by using a solvent e.g. acetone, the tape is detached. The thin flakes obtained vary in lateral dimensions in the order of tens to hundreds of micrometers as well as thickness (SLG, BLG and FLG). These flakes are identified using the contrast difference in an optical microscope. A SLG has an absorption rate of 2.3% but due to the interference-like effect, the layer can still be observed [Figure 6] using an optical microscope by placing it on top of correctly chosen thickness of SiO_2 (300 nm) silicon wafer [1]. However, a single layer graphene may completely not visible if there is a difference of even 5% different in SiO_2 thickness. Measured carrier mobilities and concentrations are up to 10,000 $cm^2v^{-1}s^{-1}$ and 10^{13} cm^{-2} respectively[3].

Although this method of synthesizing graphene is simple and cheap, do not require complicated equipment and obtained graphene with almost defect free but it has also several shortcomings such as difficult to obtain larger amount of graphene, lack of controllability, time consuming and labour intensive in identifying the SLG, BLG and FLG on the substrate surface.

Exfoliated graphene is widely used in research works for fundamental studies of transport physics and device demonstrations. It does not yet appear to be scalable to large area preparation as well as far beyond the consideration of industrial engineers.

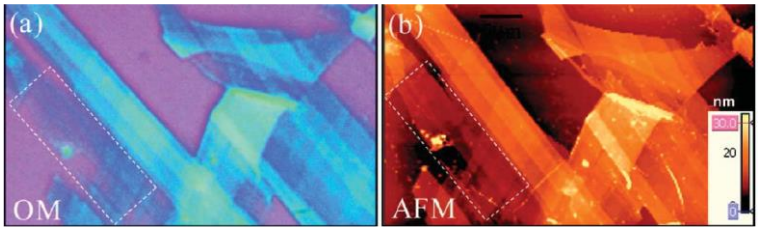

(a) (b)

Figure 6. Images of mechanically exfoliated graphite flake containing regions of different thicknesses taken by (a) an optical microscope (OM), (b) an atomic force microscope (AFM). The highlighted dashed rectangle shows a thickness of < 2 nm. Reproduced from [24].

2.4.2 Growth on Surfaces

In this method, the growth can be done in two different ways: either by readily available carbon source in the substrate or be added by a process called chemical vapour deposition (CVD).

2.4.2.1 Epitaxial Growth

This technique is commonly used for producing high quality monolayer graphene. Originally, epitaxial graphene was grown from thermal decomposition of silicon carbide (SiC). This method basically heating up bulk SiC between 1000 °C and 1500 °C in either ultrahigh vacuum (UHV) or atmospheric pressure. This heating process cause Si to sublimates from SiC substrate, leaving a thin layer of carbon behind the surface [21].

Berger C. et.al [25] demonstrated that few layer graphene can be produced from thermal decomposition of SiC. The Si face of 6H-SiC single crystal was first prepared by oxidation or H_2 etching for the purpose of surface quality improvement. Then, it was heated to 1000 °C using electron bombardment in UHV in order to remove the oxide layer. Followed by further heating up to 1450 °C, a thin graphitic layer can be obtained on the surface of the sample. Depending on the heating temperature, 1 to 3 layers were obtained. The fabricated device was measured to have a mobility of 1100 $cm^2v^{-1}s^{-1}$.

Although thermal decomposition of SiC has the potential in producing wafer scale graphene layers but it requires UHV, high temperature (up to 1600 °C) environment incurring thermal budget that prevent the technique against integration with current silicon technology. Other issues such as controlling the number of layers, interface effects with the substrate and reproducibility of the layers are also yet to be solved.

2.4.2.2 Chemical Vapour Deposition (CVD)

In CVD process, a metal is used as a catalyst and then the substrate subsequently exposed to gaseous compounds and heated under low vacuum to around 1000 °C, whereby these compounds decompose resulting in a thin film deposited on the surface of the substrate and the by-products will be removed away.

A thin layer of graphene can be synthesized by exposing a metal catalyst for example nickel (Ni) to a gas mixture of methane (CH_4), hydrogen (H_2) and argon (Ar) at about 1000 °C [23]. The CH_4 will decompose on the Ni film surface, the H_2 evaporates and the carbon diffuses into the Ni. After the growth then followed by a cooling process in an Ar atmosphere, layer of graphene can be obtained on the surface. The average number of the as-deposited layers of graphene depends on the Ni thickness and the growth time, hence can be controlled. However, because of the relatively high solubility of carbon (C) in Ni, it is difficult to completely suppress C precipitation, hence, as-growth films vary from monolayer to tens of layer.

A patterned graphene layer can be obtained by patterning the Ni layer, as shown in [Figure 7]. The as-deposited graphene layers can be transferred using polymer support, which can be attached onto the top of the graphene layer. Then after the Ni is etched, the graphene can be transferred onto the desired substrate and the polymer support is etched away. This process allows several layers of graphene can be stamped onto each other in order to decrease the resistance. The transmittance of the grown film is about 80% and the electrical measurement on fabricated structure showed an electron mobility 3750 $cm^2V^{-1}s^{-1}$ at a carrier density of ~ 5 x 10^{12} cm^{-2}.

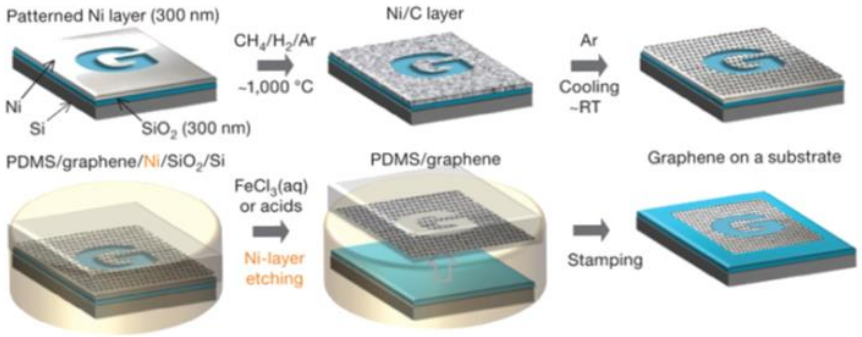

Figure 7. Synthesis of patterned graphene on thin nickel layers, etching and transfer of graphene films using a PDMS stamp. Reproduced from [23].

In another similar process, Xuesong Li et.al [9] in which copper (Cu) foils was used as a catalyst, showed about 95% of the substrate are grown with a monolayer graphene films and the rest having multi-layers graphene flakes. The graphene film thickness is independent of the Cu foil thickness and do not grow with time. This can be explained due to the fact of the low solubility of carbon in Cu or

driven by a surface catalysis effect and the process is self-limiting, that is, the growth process terminated once the Cu surface was fully covered with graphene films. The authors fabricated dual gated FETs with Al_2O_3 as the gate dielectric and extracted a carrier mobility of 4050 $cm^2V^{-1}s^{-1}$ with carrier concentration of 3.2 x 10^{11} cm^{-2}. The work explained above demonstrated a CVD method that used centimetre scale copper substrates shows a new route to large-scale production of high quality grapheme films for practical applications.

In a similar approach but in a large-scale preparation, Sukang Bae et.al.[10] has developed and demonstrated a roll-to-roll production of 30-inch graphene films for transparent electrodes using copper foil as catalyst via CVD. The synthesized graphene was transferred onto a polyethylene terephthalate (PET) substrate by roll-to-roll process [Figure 8]. The electrical properties of the graphene layer further enhanced by p-doping with nitric acid (HNO_3). The fully functional touch screen panel, a p-doped four layers graphene film stacked onto a PET substrate, has a sheet resistance of approximately 30 $\Omega.Sq^{-1}$ with about 90% optical transmittance, which is superior to indium tin oxide (ITO).

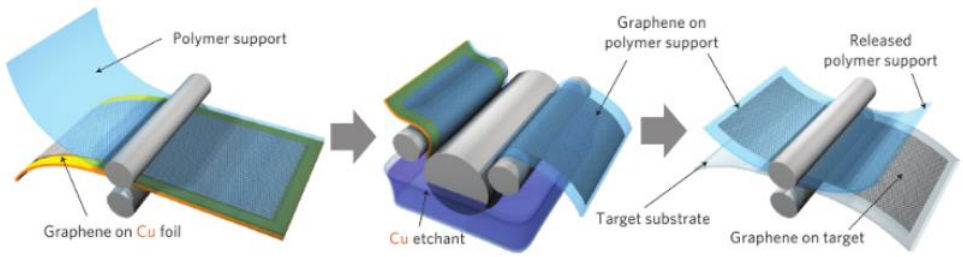

Figure 8. Roll to roll process of graphene films grown on copper foils by CVD. Reproduced from [10].

Seunghyun Lee et al.[26] have demonstrated that a uniform bilayer graphene film over an area of 2 × 2 inches using CVD on a copper substrate is feasible. The optimal growth conditions for the as-deposited films required the substrate to be heated at 1000 °C for 15 min, with a pressure of 500 mTorr, 70 sccm of CH_4 and a cooling rate of 18 °C/min. The AFM, Raman spectra and TEM used to confirm the nature of the synthesized bilayer graphene. The electrical transport measurements were conducted by fabricating dual-gated transistors with different channel lengths and channel widths and reported able to open up sizeable bandgap. The measured carrier mobility was ~ 580 $cm^2V^{-1}s^{-1}$.

However, metal catalyzed growth CVD method has several drawbacks that it requires complicated and skilled post-synthesis technique whereby as-grown layer need to be transferred either using wet/dry transfer process to desired substrates for most electronic applications. These transfer processes inevitably resulting in metal contamination, wrinkles, pinholes and breakage of the

samples, which are usually detrimental to device performance or even failure and not favourable in current Si-wafer fabrication processes.

Thus, a scalable method for reliable production of graphene layers on any insulating substrate e.g. SiO_2, S_3N_4 etc. is necessary and developed which subsequently a direct fabrication of graphene device can be made possible without transfer process of the deposited graphene.

Summary of different methods of synthesizing graphene highlighting their advantages and disadvantages are in **Table 1**.

Method	Description	Advantages	Disadvantages
Mechanically exfoliated	Graphene peeled from bulk graphite using adhesive tape	• Simple and cheap • High quality • Defect free graphene	• Time consuming • Lack of controllability (random shape , location and size) • Not scalable
Epitaxial growth	Thermal decomposition of SiC (1000-1500 °C)	• Wafer scale size • Larger grain size	• Expensive substrate • High thermal budget requirement • High vacuum required
CVD using metal catalyst	Decomposition of carbon precursor on metal catalyst e.g. nickel and copper at elevated temperatures	• Relatively low deposition temperature • Large scale size wafer is possible • Compatible with existing semiconductor	• Requires post synthesis process • Possible metal contamination • Degrade already high quality graphene
Metal catalyst free using RF-PECVD	Decomposition of hydrocarbon e.g.CH_4 without metal catalyst using RF-PECVD	• No limit on the size of substrate • No post synthesis process • Free from metal contamination	• Low quality multilayers of graphene • Small grain size

Table 1. Summary of different methods of graphene synthesis highlighting their advantages and disadvantages.

2.5 Review of Nanocrystalline Graphene on Insulator

Lianchang Zhang et.al [15, 27], reported that for the first time a new approach of synthesizing graphene directly on various substrates e.g. sapphire, quartz, mica, Si, SiC, over a large area (up to 4 inch glass wafer) without a transition metal catalyst using *r*-PECVD at relatively low temperature of 550 °C.

The sp^2 bonded honeycomb carbon structure was confirmed by Raman spectroscopy and X-ray photoemission spectroscopy (XPS). As confirmed with Scanning tunneling microscopy (STM) measurement, the as-grown films are NCG with a size of approximately tens of nanometres in lateral size.

The as-grown film on SiO_2 substrate was synthesized using CH_4 as the precursor, operating at a temperature of 550 °C at different growth durations. In the initial growth duration (2 hour), nucleated nanographene islands (~1.2-1.5 nm thick) can be observed everywhere on SiO_2 substrate shown in **Figure 9(a)** but as the growth duration increased (3-4 hours), continuous, uniform and thicker NCG film with 3-4 layers can be observed on the substrate [**Figure 9**(b) and (c)] with sheet resistances of approximately 25 kΩ and 2 kΩ respectively.

The Raman Spectra showing the characteristic of a graphitic structure of the as-grown film on SiO_2 is illustrated in Figure 9(e). The spectra shows very high intensity of the D peak, which originates from either small crystallite sizes or an abundance of edges.

The deposition time in order to achieve similar NCG coverage or sheet resistance are substrate dependant. The different in the deposition rate are speculated due to the different adsorption abilities of hydrocarbon radical on different substrate in plasma environment - low surface roughness and less mismatch substrate produced faster deposition and bigger crystal size - might be caused by different adsorption abilities of hydrocarbon radical species on different substrates in plasma.

The electrical properties of the NCG film are investigated by fabricating two terminal devices using ebeam lithography. The I-V, temperature dependence of the resistance, optical transparency/sheet resistance (quartz or glass) curves are as shown in **Figure 10**(a), (b) and (c) respectively. The linear I-V characteristics of the shows that the NCG film is a good electrical contact for adjacent nanographene interconnects, otherwise tunneling barriers with exponential I–V curves will be present.

The resistance of the NCG film has a negative temperature dependent. It is reported that this characteristic is due from the thermal generation of charge carriers at the neutrality point, while the magnitude of the change and the shape of the R–T curve are determined by electron and hole scattering and acoustic phonon.

By tuning the growth duration, the transmittance of the NCG film on quartz or glass varying between 92% and 85% having resistance of 40 and 7kΩ sq^{-1} respectively, at a wavelength around 550 nm.

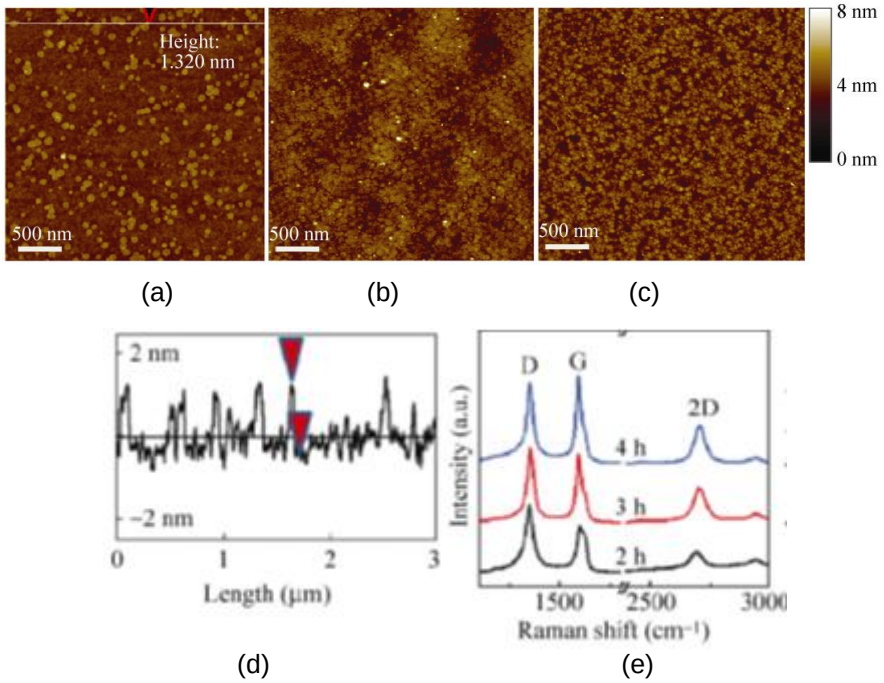

Figure 9. AFM images of different growth deposition of NCG grown on SiO_2 (a) 2 hour, (b) 3 hours, and (c) 4 hour. (d) Topography height profile along the line shown in image (a). (e) Raman spectra (excitation laser had λ =633 nm, and beam spot size ≈1 μm) of as-grown film on SiO_2 (a), (b) and (c) respectively. Reproduced from [15].

From the investigation, it shows that direct synthesizing of large area graphene onto insulators have been made possible even at low temperatures. The derived properties of the film such as the transparency with relatively low resistance might have various potential applications in the fabrication of transparent and conductive film etc.

Jie Sun et.al [28] reported that a large area uniform NCG can also be synthesized directly SiO_2/Si substrates by atmospheric pressure CVD (APCVD) without using any metal catalyst. CH_4 was used as a carbon precursor gas, mixed with auxiliary reduction, H_2 and carrier, Ar gases. The substrate was heated to 1000 °C (at a rate of 30 °C/min) under H_2 and Ar atmosphere at 50:1000 sccm respectively, kept at 1000 °C for 3 min followed by 300 sccm of CH_4 to initiate the formation of graphene. The typical growth time was 30–60 min. The residual reaction gases was removed by leaving H_2 + Ar gases to flow for further 3 min before allowing the chamber to naturally cool to room temperature (20 °C/min)

The as-grown NCG films exhibits continuous, smooth and uniform throughout the wafers with no noticeable pinhole. But some particles can be found on the surface believed to be the co-deposition

of nanographite [Figure 11(a)] during growth. The thickness of the film can be tuned by varying the deposition time and/or CH_4 pressure.

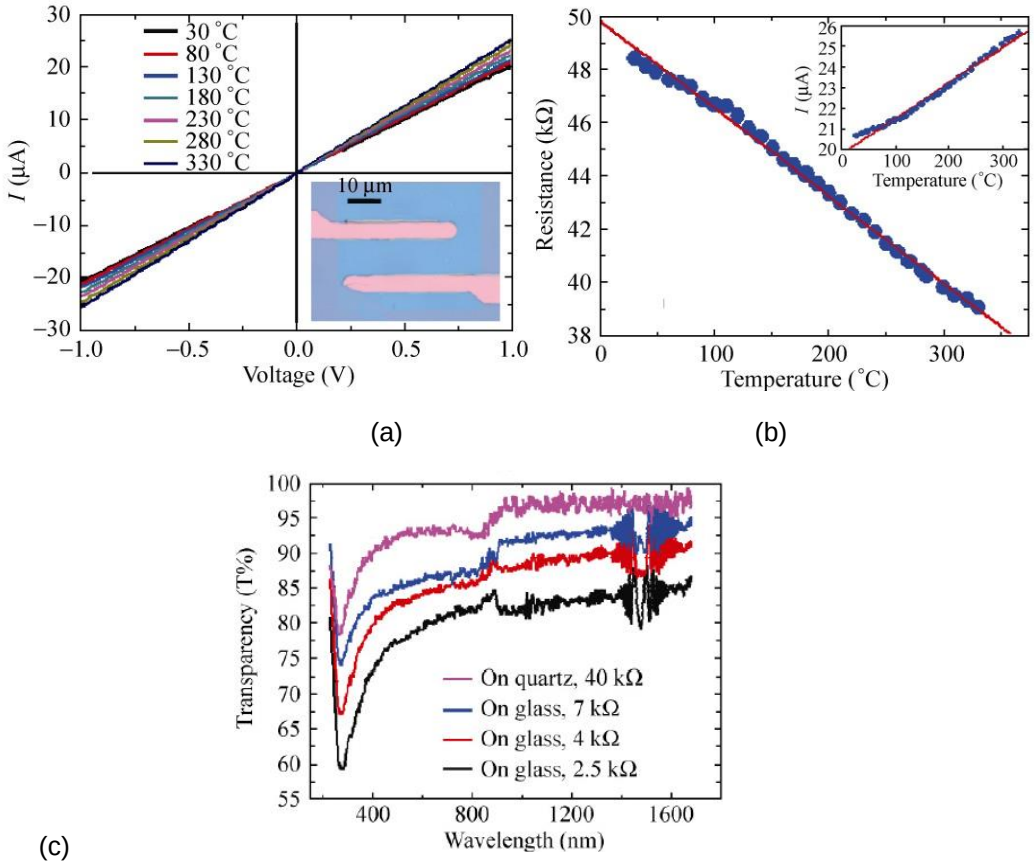

Figure 10. (a) I–V curves (b) Resistance changes at different temperatures. The red line shows a linear fit. The inset shows the I–V curve. (c) Transmittance spectra of samples with different sheet resistance. Reproduced from [15].

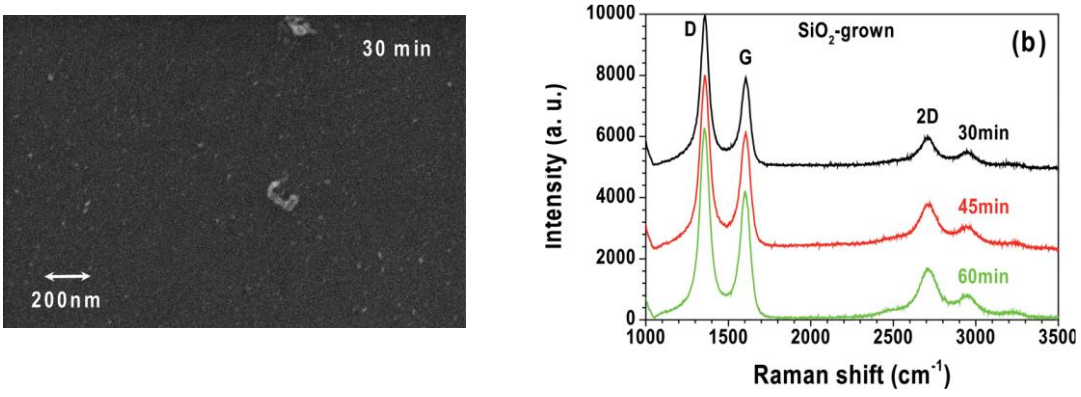

Figure 11. (a) SEM micrograph of the nanocrystalline graphene grown for 30 min directly on 300 nm SiO_2/Si, (b) Raman spectra of NCG deposited at different deposition time. Reproduced from [28].

The Raman spectra of the NCG film (**Figure 11**(b)) shows high intensity of the D peaks (or defects) with grain size approximately 10 nm. The NCG film sheet resistance as measured using four-probe indicated a range of 13.3 – 5.4 $K\Omega Sq^{-1}$ and gradually decrease as the film gets thicker. Although the film resistance is lower than as mentioned in [15], no optical transparency was mentioned.

Jie Sun et.al [29] demonstrated that graphene layers can be deposited directly on Si_3N_4 / Si at 1000 °C using APCVD without metal catalysts. The growth process can be described as self-assembly of carbon clusters from hydrocarbon pyrolysis because there was no catalytic chemical reaction involved. The as deposited film has no wrinkle and pinhole-free and termed as “graphene-like” film because of its optical as well as electrical properties similarities as of metal catalyzed graphene film. The thickness of the synthesized film can be controlled by tuning the deposition time and/or the carbon precursor pressure (CH_4). The crystallinity and carrier mobility of the as film is relatively poor compared to [28] and still requires continues optimization.

Chen et.al [13] demonstrated that they are able to obtain polycrystalline graphene on SiO_2/Si substrate by pre-annealed the substrate in flowing air prior the growth. This is speculated to remove any organic residues and activates the growth sites. After the pre-treatment step, the substrate was introduced a flow of reaction gas mixture of CH_4:H_2:Ar (14:50:65) at 1100 °C for 3 hours. Systematic studies showed that initially small graphene islands form, which grow and eventually merged to form a polycrystalline graphene layer. The number of graphene sheets produced can be controlled by tuning the carbon flow, deposition temperature or growth time. The thinnest graphene film synthesized on quartz as characterised by UV-vis spectroscopy shows transmittance of 91.2% (at 500 nm wavelength) with approximately 800 $\Omega.sq^{-1}$ sheet resistance. The sheet resistance of the graphene film with this method was much lower than [15] and [28]. Rummeli et.al. [30] demonstrated that nanographene film can be deposited directly on MgO at as low as 325 °C via CVD using acetylene as the feedstock.

From the above reviews, it clearly be seen that deposition of graphene like or NCG film have been made possible deposited directly on insulating substrate without metal catalyst. The common features of the deposition methods reviewed above show that they are operating at higher temperatures (>900 °C). At this deposition temperature, it may cause damage to other devices residing on the wafer if the graphene film is to be deposited directly on them. This suggested that for the deposition techniques to be easily adapted for use in Si based technology, low temperatures growth temperatures are required.

Research group	Substrate/ Precursor/ Synthesis method	Growth Temperature/ Time	Grain size (nm)	Sheet resistance (kΩsq-1)	Test structure (Electrical measurement)	Transmittance (@ 550 nm)
Lianchang Zhang et.al [15, 27]	CH_4 / r-PECVD	550 °C 3-4 hrs	Several tens	2.5 - 10.5	2 Terminal devices	>92 % (40 $k\Omega sq^{-1}$, on quartz) >85 % (7 $k\Omega sq^{-1}$ on glass)
Jie Sun et.al[28]	SiO_2/ CH4 / APCVD	1000 °C 30-60 mins	~10 nm (Raman)	5.4 -13.3 (four point probe)	Hall bar structure	NA
Jie Sun et.al[29]	Si_3N_4 CH_4 /APCVD	1000 °C 60-80 mins	NA	2.3 – 10.5 Hall Measurement	Hall bar structure	NA
Chen et.al [13]	SiO_2/Quartz CH_4/ Oxygen aided APCVD	1100 °C 3 hrs	NA	Carrier mobility 531cm^2/Vs	FET	91.2 % (800 Ωsq^{-1}, on quartz) 63.5 % (210 Ωsq-1, on quartz)
Rummeli et.al[30]	MgO/ Acetylene / CVD	325 °C Up to 2hrs	50 nm (Equation) 30 nm (Raman) 2-5 nm (TEM)	NA	NA	NA
Jie Sun et.al[14]	Quartz/Sapphire CH_4 / Thermal CVD	1000 °C	10 nm (TEM)	2.9 (on quartz) 13 (on sapphire)	Hall bar	~ 97%

Continue

Table 2. Summary of research groups working on different growth conditions and measured properties of NCG grown directly onto insulating substrates.

Continued

Henry Medina et.al [12]	SiO_2 C_2H_4 ERC-CVD	400 °C	2 -3 nm (Equation) 3-5 nm (TEM)	20 (on glass)	FET	~94%
Kalita et.al[31]	Si and SiO2 C_2H_2 SWPCVD	400 - 560 °C 70-120 sec	80-100 nm	6.8	Photovoltaic device	0.82
Marek E. Schmidt et.al[32]	SiO_2/Quartz/Sapphire CH_4/ PECVD	750 - 900 °C 1-15 mins	1.74-2.67 nm	3.73	Bar strips	>85%

Table 2. Summary of research groups working on different growth conditions and measured properties of NCG grown directly onto insulating substrates (cont.).

2.6 Review of Transparent Conductor with Graphene

Jie Sun et.al.[14] synthesized graphene film directly on quartz and sapphire to demonstrate the potential of transfer free NCG film graphene based transparent electrodes application.

The NCG film obtained clearly shows the G band and 2D band, with high intensity of D-peak that exhibit defects in the crystallites. **Figure 12** shows the transmittance spectra of the NCG film showing an independent of the light wavelength. The film has a sheet resistance of 2.9 kΩ and 13 kΩ for quartz and sapphire respectively.

.

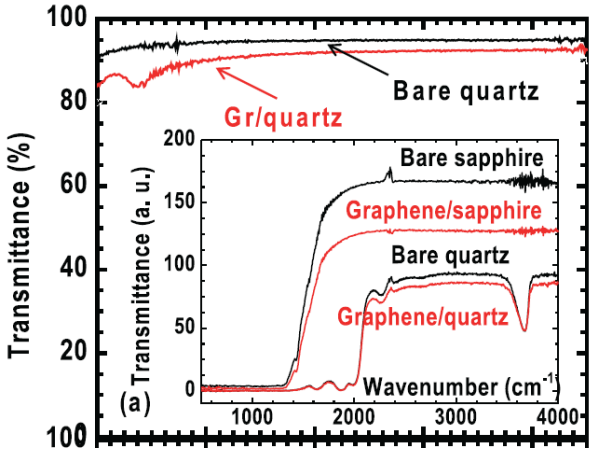

Figure 12. Transmittance spectra of the NCG on quartz. Reproduced from [14].

Henry Medina et.al [12] *r*eported that a direct growth of continuous large area flat nanographene films on silicon oxides is possible at a temperature greater than 400 °C using electron cyclotron resonance (ERC) CVD without a metal catalyst. Their work confirmed similar works by [15, 28, 30] that NCG films can be directly grown on insulating substrates such as SiN, Si, Al_2O_3 and SiO_2, as per confirmed according to their Raman spectra with common features of fairly low 2D and overlap D and G peaks (poor crystalline quality). The high intensity of D peak as reported is due to the plasma as well large density of domain boundaries of the film. The estimated domain size L_a, yields an average domain size of 2-3 nm.

$$\frac{I_D}{I_G} = \frac{C(\lambda)}{L_a} \quad [12] \qquad \textbf{Equation 1}$$

Where $C(\lambda) = C_0 + \lambda C_1$

$$C_0 = -12.6nm$$
$$C_1 = 0.033 \text{ (constant valid for } 400 < \lambda < 700 \text{ nm)}$$

Where $\frac{I_D}{I_G}$ *is the ratio of the D over G peak intensity and λ is the laser excitation wavelength.*

The optical transmittance and sheet resistance of their thinnest film grown on glass [**Figure 13(a)** and (**b**) respectively] show 94% (at 550 nm excitation wavelength) and approximately 20 kΩ.sq^{-1} respectively. The resistance drops as the growth time increases (thicker film). Further acid treatment in HCl aqueous solution and functionalization in $SOCl_2$ reduced the sheet resistance.

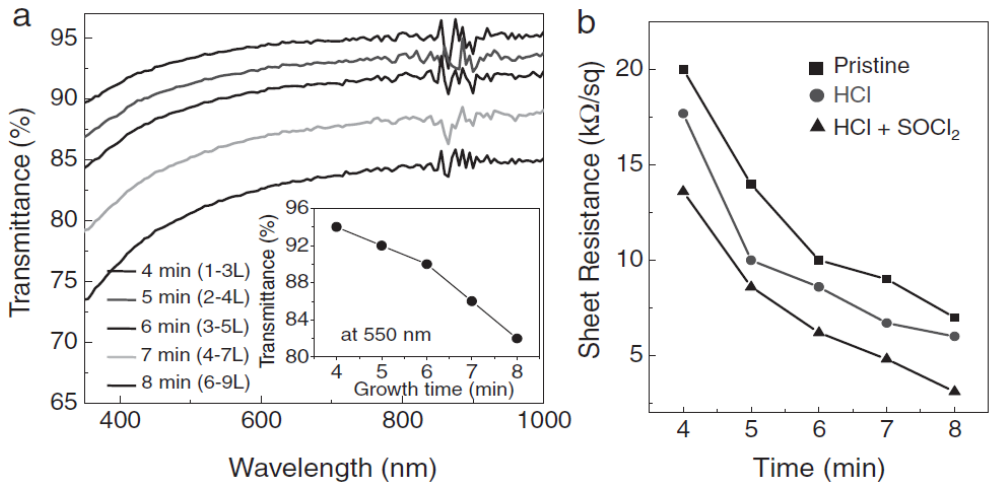

Figure 13. (a) Optical transmittance of ECR-CVD nanographene grown on quartz, with different film thickness. The inset compares the transmittance at 550 nm for different growth durations. (b) The sheet resistance decreases as the film thickness increases; further resistance reduction when doped by chemical functionalization in HCl and $SOCl_2$ aqueous solutions. Reproduced from [12].

Kalita et. al. [31] reported that they successfully synthesized nanographene film directly on silicon and glass without metal catalyst using microwave assisted surface wave plasma (MW-SWP) CVD at reaction temperatures between 400 °C and 560 °C. The synthesized nanographene film consists of triangular shaped domains with sizes of 80–100 nm in length. The nanographene domains observed were interconnected which formed a continuous film with metallic behaviour. The film deposited at 560 °C has better crystallinity compared at those lower reaction temperatures. The transmittance and sheet resistance of the film were 82% (at a wavelength of 550 nm) and 6.8 kΩ sq^{-1} respectively. The high sheet resistance reported was due to the nanosized domains.

Marek E' Smith et al [32] reported that NCG can be deposited directly onto SiO_2, sapphire and quartz using PECVD without metal catalyst. The uniformity of NCG deposited on 150mm wafer was as low

as 13%. The sheet resistance R_{sq} and charge carrier mobility μ were 3.73 kΩ and 2.49 $cm^2 V^{-1}s^{-1}$ respectively. The NCG film on quartz and sapphire has >85% optical transparency in the visible range and their sheet resistance was still relatively high in the range of 2.5 kΩ - 7.5 MΩ. It was reported that no further investigation was conducted to lower the sheet resistance but the metallic properties of the film make them suitable for transparent electrode applications.

Although the NCG film synthesized in [12, 14, 32] need further optimization, it was reported that the growth film has potential application in transparent conductive electrodes, electrical interconnects, interference shielding and other electronic devices.

2.7 Review of Transparent Conductor and its Criteria

Transparent conductors/electrodes (TC) are widely used in many applications such as low emissivity windows in buildings, transparent electromagnetic shields, windows for displays, touch screen technologies [33] and thin film photovoltaics for renewable energy applications.

The minimum standards required for transparent conducting material to be industrially accepted are the sheet resistance should be <100 Ωsq^{-1} and >90% transmittance in the visible range. Depending on the application, the requirement varies, for example, touch screen and flat panel displays applications require sheet resistance of <500 Ωsq^{-1} and approximately 10 Ωsq^{-1} [34] respectively. Mechanical strength chemical stability, the etchability, work function, the cost for raw material and processing are other additional requirement for TC [33].

Tin-doped indium oxide (ITO) is one of the widely used TCs with reported commercial specification of 0.04% absorption coefficient (highly transparent) and sheet resistance of 6 Ωsq^{-1}. ITO thin film transmittance <90% typically exhibits 30-80 Ωsq^{-1} sheet resistance. The trend towards flexible touch screens and solar technologies require bendable TCs. However, the high price, scarcity, ceramic and brittleness nature of ITO makes it unsuitable for the bendable application.

Aluminium (Al-) and Gallium (Ga-) doped ZnO are another alternatives replacement to ITO due to their low material cost and easy etching process. However, these materials have their own limitation as well such as degradation of electronic properties during processing and thicker film is required in order to achieve similar sheet resistance of ITO which in turn adding additional material cost.

Considering the limitation of metal oxide mentioned above, it highlights the need to look for new or alternative replacement of existing TC materials. The new materials should be sustainable, better performance in terms of their properties such as highly conductive, optically transparent and reasonably cheap in their production.

Among other potential materials for TCs that have been considered as the new generation TCs for electrode applications are metallic nanostructures (silver nanowires), conducting polymer, carbon

nanotubes and graphene. All of these materials are flexible with transparencies and sheet resistances comparable to that of ITO. The sheet resistance and optical transmittance of some of these emerging materials is summarised in **Table 3**.

Graphene is one of the novel TCs which has been proposed as the new generation TC for electrode application [35] due to the combination of its high charge carrier mobility, high optical transparency in the visible region, its flexibility and stretch ability. Although, graphene-based electrodes have the potential to be real low cost alternatives to ITO and their applications has been shown in research but the quality and reproducibility of graphene materials remains questionable. Eventhough there are variety of new transparent conducting electrodes under research, a total replacement to ITO will not come soon in the near future.

Metal catalyst CVD grown graphene typically at above 800 °C probably the best synthesising method of producing high quality large area graphene. If these graphene to be considered for application as transparent electrodes, additional transfer steps that is, transfer them onto transparent substrate such as polymer or glass, need to be done. Eventually, unavoidable contamination and time consuming will happen. Hence, another method of synthesising graphene such as direct synthesis of graphene on target transparent substrates such as glass or polymer at lower temperatures needs to be developed.

Research Group	Type of TCE Materials	Optical Transmittance (%) @550 nm	Sheet resistance ($\Omega.Sq^{-1}$)
[36]	Bromine within FLG	98	180
[37]	UV PET/PEDOT:PSS	52	81
[38]	Hybrid Cu mesh	91	6.197
[39]	Ag nanomesh/ZnO hybrid	88	15
[40]	Graphene on quartz	91	1300

Table 3. Summary of the sheet resistance and optical transmittance of some of emerging TCE materials.

2.8 Conclusion

In this chapter, different aspects related to graphene were reviewed. Advantages and disadvantages of several methods of obtaining graphene was compared. Several research group, have attempted to develop alternative growth methods in order to avoid drawbacks such post deposition transfer, by depositing graphene film directly onto an insulating substrates such as SiO_2, but the quality is still far from pristine or metal catalysed CVD graphene and hence, new findings and branch of research in this field is still feasible.

Some criteria required for the materials to be considered as transparent conductor applications was also reviewed.

CHAPTER 3
PECVD Process and Carbon Deposition

This chapter outlines briefly what a chemical vapour deposition (CVD) is, and different type of CVDs. Some of their advantages and disadvantages is also summarised. PECVD deposition principle is also explained briefly.

3.1 Introduction of CVD

Generally, chemical vapour deposition (CVD) is a deposition process in which chemical precursors are transported in the vapour (gas) phase to decompose on a heated substrate and eventually turn into a solid material in a form of thin film. In a typical CVD process, the substrate is exposed to one or more volatile precursors, which eventually react and/or decompose on the substrate surface to produce the wanted deposit. The process also produces volatile by-products (may be toxic), which are then removed by gas flow through the reaction chamber.

CVD is widely used in semiconductor industry as part of the device fabrication processes, also to deposit various films which may be epitaxial, polycrystalline or amorphous depending on the materials e.g. silicon and carbon nanotubes, and chamber conditions. CVD gained its popularity for deposition of film in semiconductor industry mainly because of its high throughput, high purity, and low cost of operation. Optoelectronics application is one of many examples where CVD is widely used.

Some of advantages and disadvantages of CVD over physical vapour deposition (PVD) such as molecular beam evaporation are as follows:

> *Advantages:* CVD pressure allows coating of three-dimensional structures with large aspect ratios, meanwhile PVD are typically line of sight depositions (may not give complete coverage); high precursor flow rates allows faster deposition rate; simple and scalable reactor to accommodate several substrates; do not require UHV and easy changes of precursor.
>
> *Disadvantages:* high deposition temperatures (above 600 °C) which is unsuitable for fabricated device; precursor and by-products may be hazardous or toxic; many process parameters to be tuned or optimise for reproducibly deposit good films.

There are a number of CVD system widely used and referenced in the literature, and classified on the basic by which chemical reaction are initiated for example activation process, and process conditions. Amongst available CVD systems are briefly discussed below.

3.1.1 Atmospheric pressure CVD (APCVD), Low pressure CVD(LPCVD) and Ultrahigh vacuum CVD(UHVCVD), whereby CVD processes are conducted at atmospheric pressure, sub atmospheric and very low pressure (typically below 10^{-8} torr).

3.1.2 Atomic layer CVD (ALCVD) or atomic layer deposition (ALD), whereby two complementary precursors are alternatively pumped into the reaction chamber.

3.1.3 Hot wire CVD (HWCVD) or Hot filament (HFCVD) whereby CVD process utilizes hot filament to decompose the precursors.

3.1.4 Microwave plasma-assisted CVD (MPCVD), whereby CVD process utilizes microwave power to decompose precursors to sustain plasma.

3.1.5 Plasma enhanced CVD (PECVD), whereby CVD process utilizes plasma to enhance chemical reaction rate of the precursors that allows lower deposition temperature.

3.1.6 Remote plasma enhanced CVD (RPECVD), similar principle to PECVD but the sample is placed away from the plasma discharge region - enables deposition temperature down to room temperature.

3.2 Principle of Plasma-enhanced CVD (PECVD)

PECVD or plasma-assisted (PACVD) is another variant of CVD whereby chemical reactions activated only after creation of a plasma of the reacting gases. The plasma is generally created by radio frequency (RF) / alternating current (AC) or direct current (DC) discharge between two electrodes and the space between these electrodes is filled with the reacting gases.

Figure 14 illustrates the reaction sequence in PECVD. Plasma (electrically conductive) is a partially ionized gas consisting of free electrons and ions and neutral atoms and is formed when sufficient energy is introduced into a gas. The mass of electron is much lighter than ion hence accelerated faster to the changes in the RF field but they do not increase the temperature of the plasma. Since ions cannot respond quickly to the changes in direction, hence keeps temperature low.

Electron energies in the plasma have a Maxwellian distribution in the range of 0.1 to 20 eV, sufficient to excite molecules or break chemical bonds in collisions between electrons and gas molecules

resulting in excitation or ionization. The reactive species generated by the collisions do not have the energy barriers to reactions that the parent precursors do. Therefore, the reactive ions are able to form film at temperatures much lower than those required for thermal CVD.

The reactive species resulting from electron dissociation of precursor molecules also diffuse to the surface. The reactive species have lower activation energies for chemical reactions and usually have higher sticking coefficients to the substrate. Hence, PECVD reaction is controlled by the reactive species on the surface.

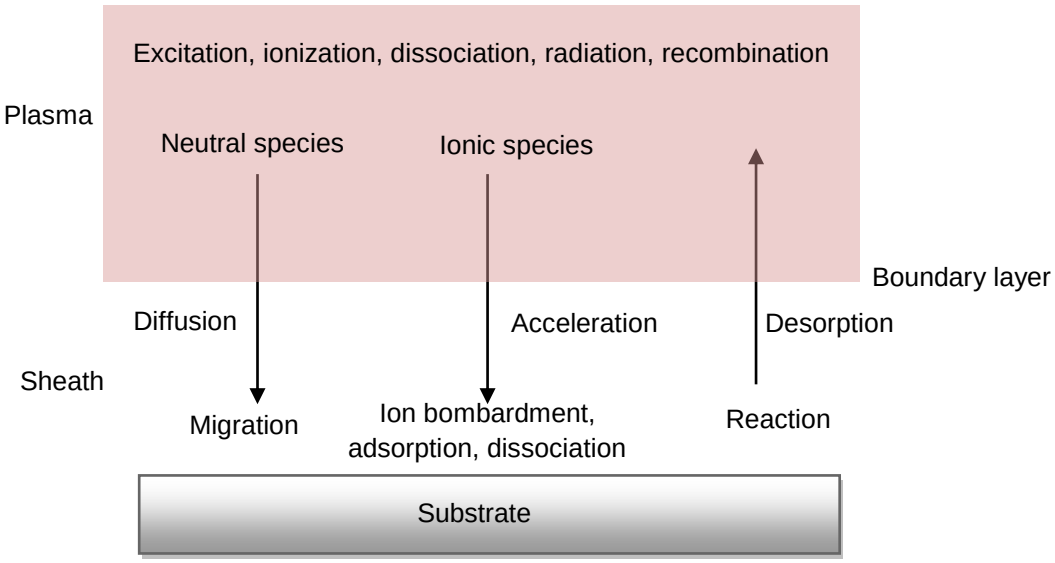

Figure 14. Reaction sequence in PECVD. Reproduced from [41].

PECVD is widely used to deposit thin film such as silicon dioxide, silicon nitride, diamond like carbon (DLC), Amorphous Silicon, and Poly Silicon on the semiconductor with temperature sensitive devices or structures.

In the next section below, a brief summary of advantages and disadvantages of PECVD over thermal CVD are outlined.

3.2.1 *Advantages*

Since plasma is the essential component used in the system, it helps chemical reaction or deposition occur at much lower deposition temperatures which is an advantage for temperature sensitive material in which their properties changed at higher temperatures. Meanwhile the low pressure between 0.1–10 torr is required for sustaining a plasma resulting deposition of good film uniformity.

3.2.2 *Disadvantages*

The plasma ion bombardment during the deposition process could damage the deposited film, hence, deteriorating the already fabricated device. Another disadvantage is that hydrogen in plasma nitrides always present in plasma gas. The hydrogen can react with silicon or nitrogen to form Si-H and SiNH and eventually affect many properties of the devices such as electrical conductivity, mechanical stress etc.

3.3 OIPT 1000 Agile PECVD System

Description of the system chamber and reaction chemistry

In this work, an OIPT Nanofab 1000 agile PECVD system is used for the deposition of the NCG film. The system and schematic illustration of the system process chamber is as shown in **Figure 15.**

The vacuum chamber has a parallel electrode configuration: top electrode RF driven (MHz and/or kHz) and bottom electrode where the substrate sits is grounded. These electrodes are used to generate the desired RF field and plasma is localised between them. The wafer substrate is placed on the lower electrode, which sits on top of the electrical heating element, and the temperature setting is measured and controlled by a thermocouple. The process gases are fed into the process chamber via the showerhead in the top electrode and the mass flow controllers (MFCs) control the flow rate. The chamber pressure is controlled by a butterfly valve.

The two most popular gases used as carbon precursors are methane (CH_4) and acetylene (C_2H_2). CH_4 is a popular precursor gas because it is safe to use and is the main component of natural gas. In comparison, C_2H_2 is less safe to use but it has two carbon atoms per molecules instead of one as in CH_4. In this study, CH_4 is used, as it is readily available in Southampton Nanofabrication centre.

CH_4 gas is used as the carbon precursor, which is then fed into the system chamber after the ignition of H_2 plasma by an electrical field at RF frequency of 13.56 MHz. In the process chamber, the plasma electrons collide with the CH_4 molecules and eventually decompose the CH_4 into several reactive radicals as illustrated below.

$$\text{RF Plasma } (H_2) \quad + \quad CH_4 \longrightarrow CH_x,\ C_2H_y,\ C_3H_z,\ H$$

These reactive radicals play an important role in the film nucleation and growth stages. The carbon containing radicals adsorbs (accumulates) onto the surface of the substrate and bonds with each other by diffusion and collision to form the film.

However, the RF power, reaction time and temperatures, gases mixture and pressure amongst other deposition parameters that needs to be optimised and controlled for the right reactive species formation and subsequently deposited of the film on the substrate.

Since there are, a few variable deposition parameters need to be tuned, so in this work, the following approach for synthesis of NCG film is planned by fixing and varying the parameters. This is to investigate the effect of different parameters on the quality of the deposited film. Ellipsometry, Raman Spectra and four-point probe will evaluate the deposited films.

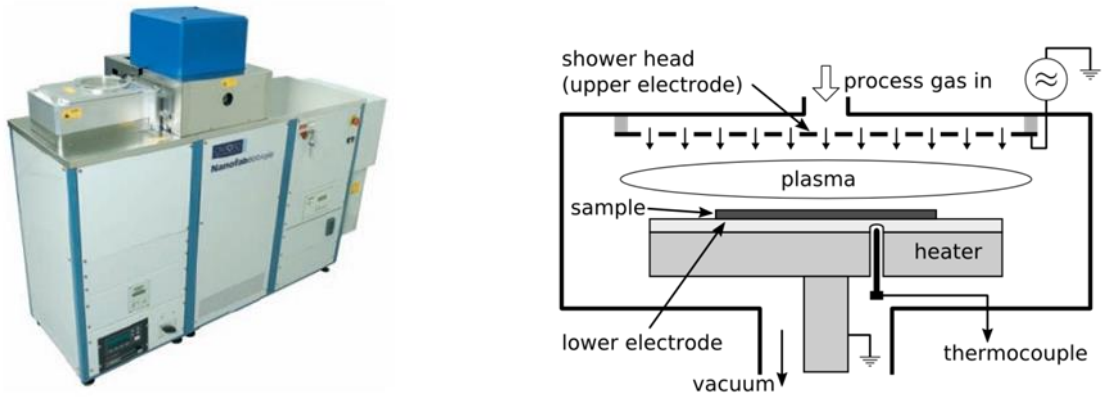

(a) (b)

Figure 15. (a) Oxford Instrument Nanofab Agile 1000 system, (b) Schematic illustration of the system chamber. Reproduced from Oxford-instruments.com

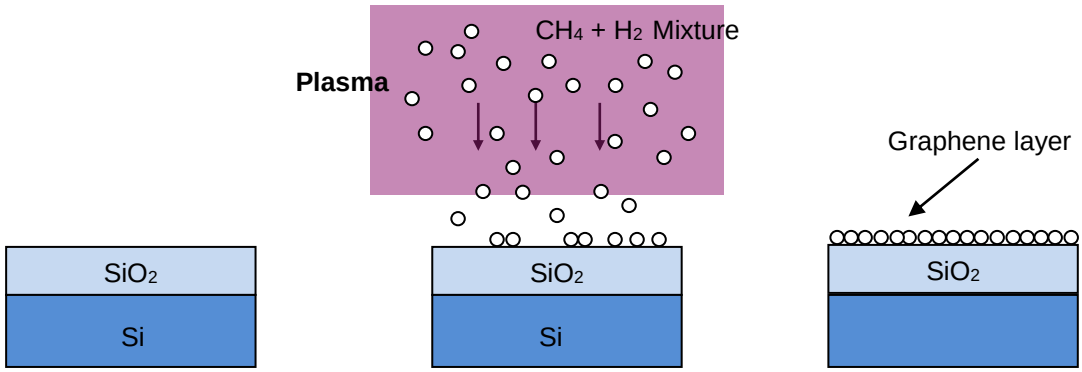

(a) (b) (c)

Figure 16. Schematic illustration of the direct deposition of nanocrystalline graphene (NCG) on an insulating substrate (SiO_2) using RF-PECVD. (a) a bare 300nm thick thermally grown SiO_2 on silicon substrate, (b) a process of RF-PECVD is taking place, (c) Diffusion of carbon atoms and later graphene layers formed on SiO_2 .

The basic concept of depositing NCG layers directly on SiO_2/Si substrate using RF–PECVD is shown as in **Figure 16** above. The deposition of NCG was realised by decomposition of gases mixture of CH_4 and H_2 in a RF-PECVD system.

3.4 Conclusion

In this chapter, a brief introduction and different types of CVD are summarised. Then some basic principle of PECVD system and differences against thermal CVD are discussed.

CHAPTER 4

Experiment and Results

This chapter outlined the RF-PECVD deposition process, parameters and characterisation of the NCG films. The deposition of the NCG film was carried out using Oxford instrument Plasma Technology (OIPT) Nanofab 1000 agile PECVD system which basically can accommodate up to 200 mm wafer and can be heated up to 1000 °C.

In this work, a 300 nm thick thermally oxidized SiO_2 on 150 mm diameter n-type silicon wafer was used to deposit NCG film at temperature ranging from 600 °C to 850 °C. Although the heating stage of the tool can reach up to 1000 °C but it was decided NO experiment to be carried out towards the maximum temperature of the system (1000 °C) due to safety reasons and other technical limitation of the system. Moreover, one of the objectives of this work is to synthesize NCG film as low deposition temperature as possible.

The first part of the work is to investigate the effect of the deposition temperature on the as-deposited NCG film while keeping other growth conditions such as deposition time, gas composition or flow rate, pressure and RF power unchanged.

Following the deposition process, the as-deposited NCG film thickness, sheet resistance and Raman spectra are characterised accordingly using Ellipsometry spectroscopy, four-point probe and Raman Spectroscopy respectively.

4.1 Deposition Process

The illustration of the deposition process is shown as **Figure 17**.

- All wafers were loaded from a loadlock chamber at a loading temperature, T_{Load}, of 650 °C to the process chamber at the desired deposition temperature, T_{Dep}, ranging from 600 °C to 850 °C.
  The time, $t_{Heat\text{-}up}$ taken to reach T_{Dep} depend on the desired deposition temperature with an approximately heating rate of 15 °C/min.

- At T_{Dep}, the wafers were annealed, t_{anneal} in H_2 atmosphere at a flow rate of 75 sccm, 1.5T pressure for 3 minutes.

This duration enables a steady flow of H_2 in the chamber and helps to remove any organic contamination and smoothen the wafer surface as well as ensures the desired temperature of the wafer has been reached.

- Then, H_2 and CH_4 plasma was struck for 60 sec (t_{Plasma}) in order to get a stable plasma strike before the actual deposition time, $t_{Deposition}$ was activated.

- Subsequently, deposition time, $t_{Deposition}$ was set to 60 minutes.

- Once $t_{Deposition}$ was completed, the plasma and process gases was halted.

- Finally, the chamber was ramped down back to the initial T_{Load}, at a rate of approximately 15 °C/min before the wafers can be unloaded from the process chamber to loadlock chamber.

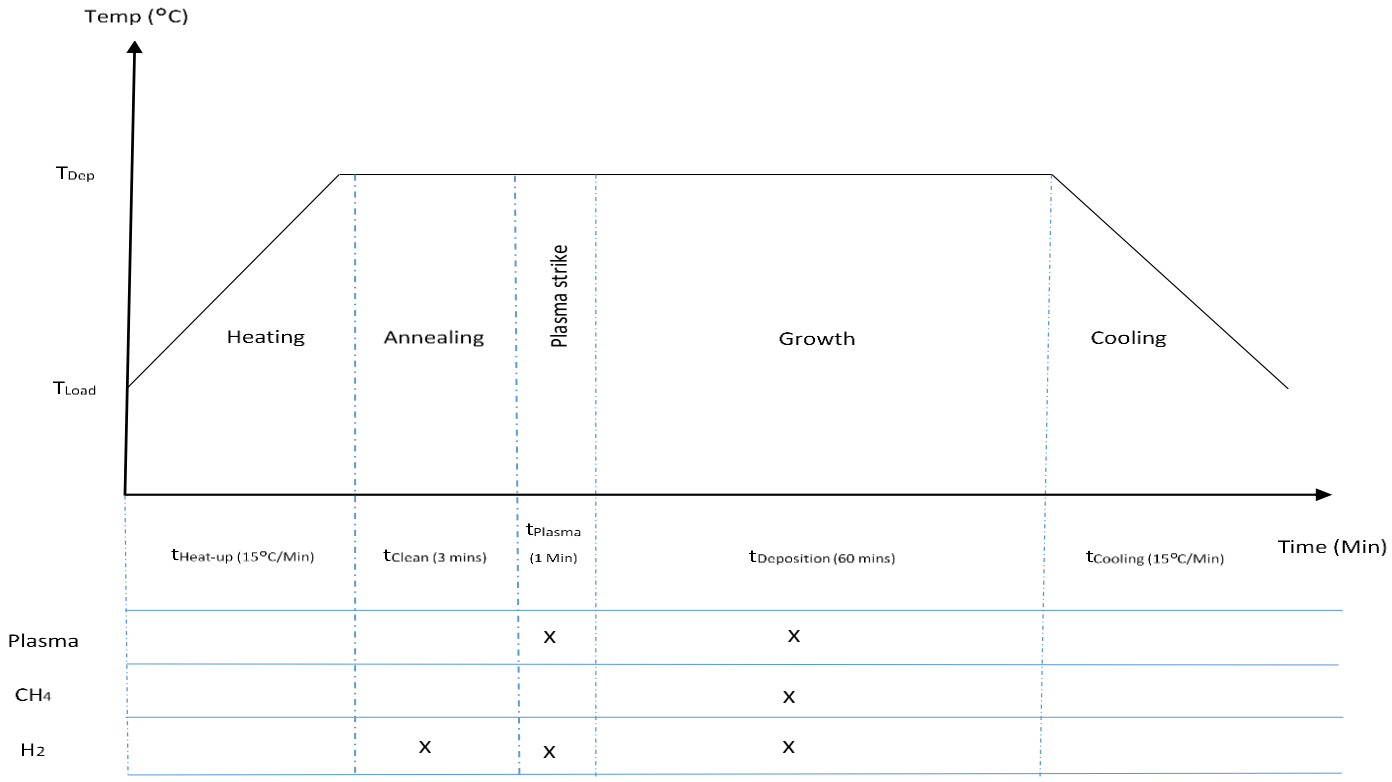

Figure 17. Illustration of PECVD deposition process of nanocrystalline graphene (NCG) film.

4.2 Deposition Parameters

The synthesis of the NCG films were based on a mixture of process gases CH_4 and H_2 at a pressure of 1.5T with RF power of 100 W. Table 3 shows the detailed experimental parameters used in the deposition of the NCG film.

In this part of the work, only the deposition temperature was varied between 600-850 °C, keeping other parameters unchanged. This was done to investigate the effect of different growth temperature on as-deposited NCG film.

Sample identifier	Temperature, T_{dep} (°C)	Pressure (torr)	CH_4 (sccm)	H_2 (sccm)	RF Power (watt)	Time, t_{dep} (minute)
$TSiO_2$ x10	850	1.5	60	75	100	60
$TSiO_2$ x11	800	1.5	60	75	100	60
$TSiO_2$ x12	750	1.5	60	75	100	60
$TSiO_2$ x13	700	1.5	60	75	100	60
$TSiO_2$ x14	650	1.5	60	75	100	60
$TSiO_2$ x15	600	1.5	60	75	100	60

Table 4. The experimental parameters for the NCG Film deposition at varying deposition temperatures, while other conditions were kept unchanged.

4.3 Characterisation of NCG film thickness and uniformity

A film thickness is one of the most important characteristic and thickness measurement is vital in investigation of a thin film. The electrical and optical properties and behaviour depends on the thickness of the thin film. In some applications such as protective and coating, the actual thickness is not of great important, but precise and reproducible film thickness is required in microelectronic application.

In this work, initially the thickness of as-deposited NCG film on SiO_2/Si sample was measured using Profilometer and Ellipsometer techniques. Then the result of these two techniques were compared for verification if the readings were comparable or not.

4.3.1 Thickness measurement using Stylus Profilometer

Firstly, one of the as-deposited NCG sample (deposited at 750 °C) was RIE etched so that a 'step' can be created as shown in **Figure 18**. Then, the profilometer measurement was conducted and later the result was verified with ellipsometer result as in **Table 5**.

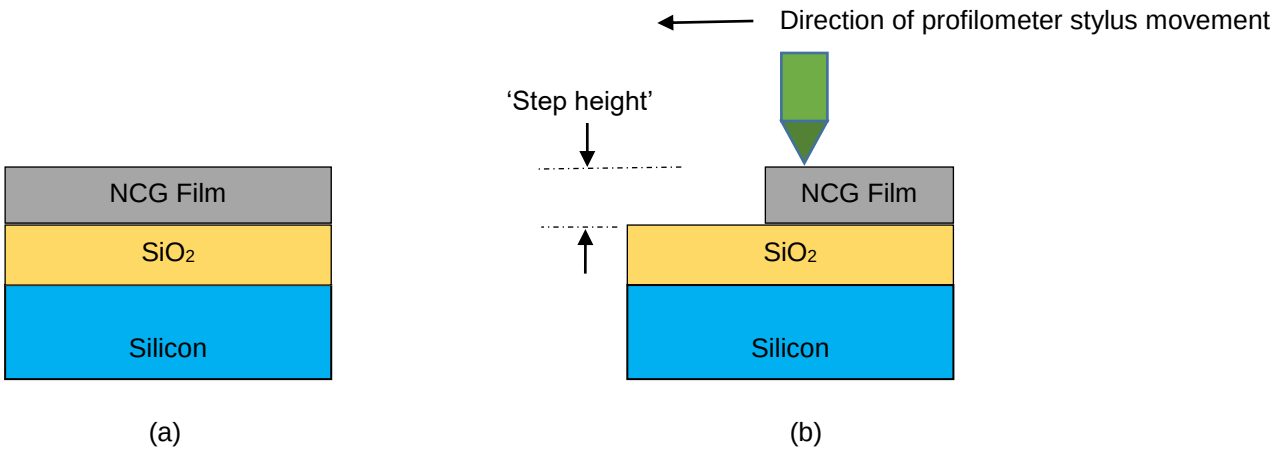

Figure 18. Schematic illustration of a method used to measure the NCG film thickness using profilometer stylus. (a) before, and (b) after 'a step' was created by RIE Etching technique.

4.3.2 Thickness measurement using Spectroscopy Ellipsometer

Ellipsometer is mainly used to determine film thickness and optical constants. It measures the changes in the polarization of a reflected light from a material surface and represented as an amplitude ratio, Ψ (psi), and the phase difference, Δ (delta). The results depend on optical properties and thickness of individual material. This method is a non-destructive and fast depending on the total number of measured points. However, this method relies on the constructed model that used to represent the material under study.

Here, the thickness and uniformity of the NCG film samples were obtained by mapping each wafer with 180 evenly spaced points using Variable Angle Spectroscopic Ellipsometry (VASE) J.A Woolam M-2000, employing a white light source.

First, the ellipsometry result of the NCG sample deposited at 750 °C was fitted using ellipsometry software (CompleteEASE) which was modelled as an absorbing material(B-Spline) on an under-laying SiO_2 and silicon substrate (as depicted in **Figure 19**) with a known physical thickness of NCG film obtained from profilometer measurement in 4.3.1.

The resulting optical constant (refractive index, *n* and extension coefficient, *k*) of the NCG film sample deposited at 750 °C used in the profilometer measurement was obtained and depicted as in **Figure 20**. Then, this characteristic was compared with other optical constant of multilayer graphene obtained from other literatures and found the optical constant was in close agreement with the one reported by [42].

Finally, both thicknesses derived from ellipsometer and profilometer measurements was compared and both showed comparable and in agreement with each other [**Table 5**]. Hence, the derived optical constant of the NCG film model was considered valid and was used to characterise the thickness and uniformity of the rest of samples with confidence. For accurate results all fitting in ellipsometry measurements, the mean square error (MSE) was kept as low as possible.

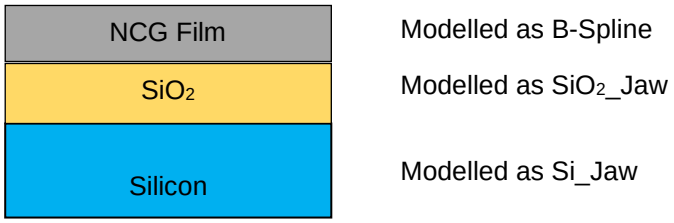

Figure 19. Ellipsometry model used to represent the NCG film on SiO_2 / Si substrate.

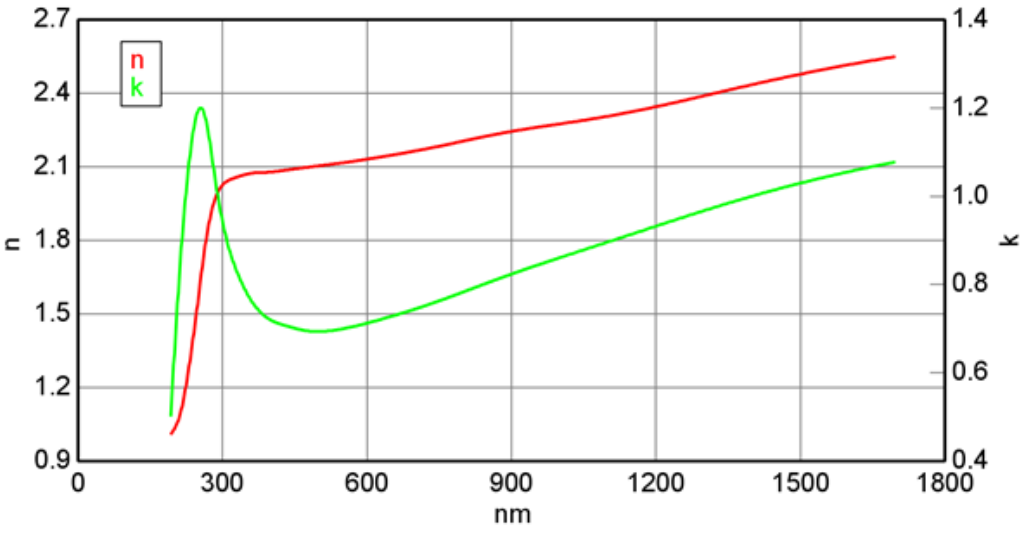

Figure 20. Optical constant of the NCG film derived from the ellipsometer measurement of NCG sample deposited at 750 °C.

Sample identifier	T_{dep} (°C)	Profilometer Thickness (nm)	Ellipsometer Thickness (nm)
$TSiO_2$ x 12	750	103	109

Table 5. NCG film thickness of sample deposited at 750 °C measured using profilometer and ellipsometer techniques.

4.3.3 Thickness Results

For consistent deposition rate calculation, only NCG film thickness on the left-centre side (approximately 3 cm from edge) of all wafers was considered. This part of the wafer exhibits uniform deposition pattern and common to all NCG samples deposited at different temperatures. In addition, around these areas transmission line measurement (TLM) structures were fabricated. The non-uniformity of the NCG deposition was due to the inclusion of small quartz sample being positioned in the middle part of the wafer. Better uniformity of as-deposited film on a wafer when there was no quartz sample.

Figure 21 shows ellipsometer measurement results on the NCG film thickness and uniformity deposited at different growth temperatures. All measurement result and derivation was shown in **Table 6**.

Sample identifier	T_{dep} (°C)	t_{dep} (Minute)	Deposition rate (nm/min)	Thickness (nm)	(Four point probe) Sheet resistance ($\Omega.Sq^{-1}$)
$TSiO_2$ x 10	850	60	3.050	183	394
$TSiO_2$ x 11	800	60	2.467	148	660
$TSiO_2$ x 12	750	60	1.817	109	1113
$TSiO_2$ x 13	700	60	1.000	60	2394
$TSiO_2$ x 14	650	60	0.046	2.75	undefined
$TSiO_2$ x 15	600	60	0.012	0.71	undefined

Table 6. Summary of the as-deposited NCG film measured thickness, sheet resistances (as measured using four-point probe) and deposition rates at different growth temperatures. *undefined – unable to obtain the reading due to very little deposition.

4.3.4 Measurement of Sheet Resistance

A simple four-point probe (Jandell Model Rm-AR) was used to measure the sheet resistance of deposited NCG films and the result was shown in **Table 6** above. The sheet resistance of the NCG films obtained from four-point probe measurement will be compared against with the results obtained from TLM technique as described in section 4.4.

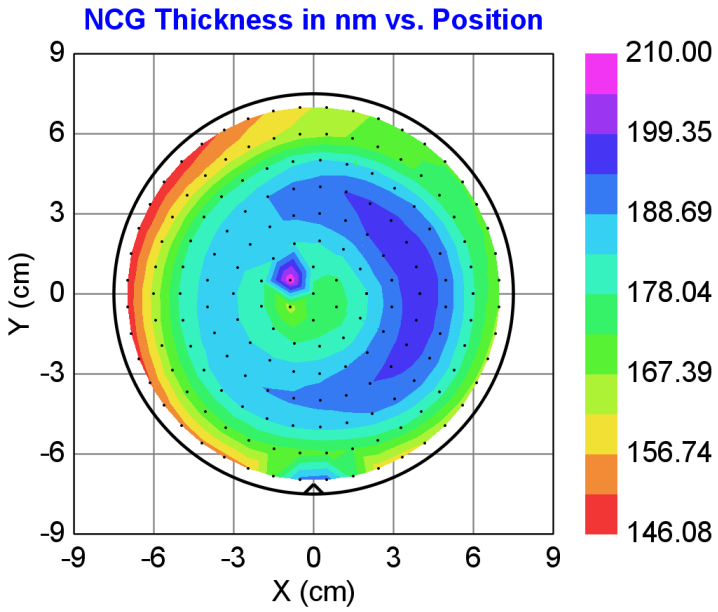

Figure 21. (a) $TSiO_2$ x10 (850 °C) with approximate NCG thickness between 160 nm to 200 nm.

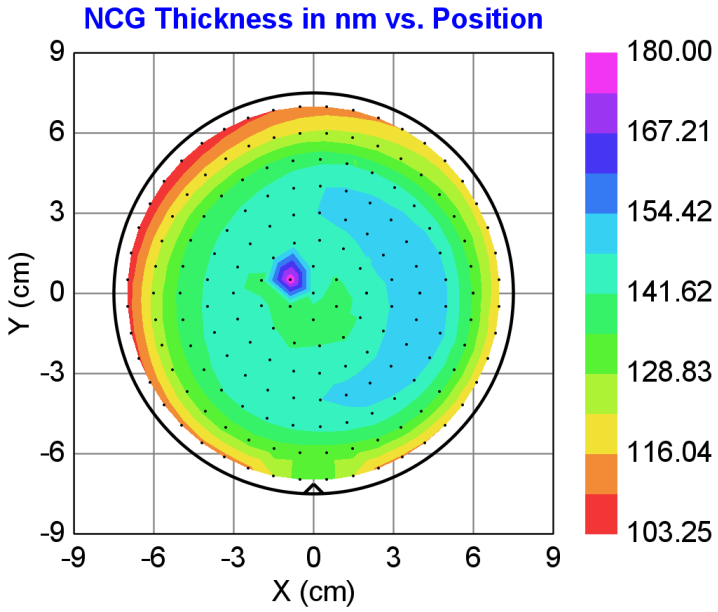

(b) $TSiO_2$ x11 (800 °C) with approximate NCG thickness between 116nm to 154 nm.

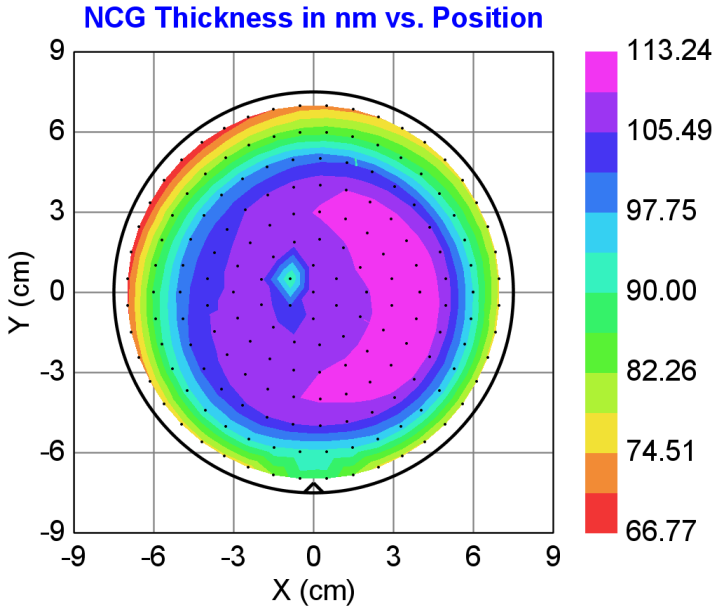

(c) $TSiO_2$ x12 (750 °C) with approximate NCG thickness between 80 nm to 113 nm.

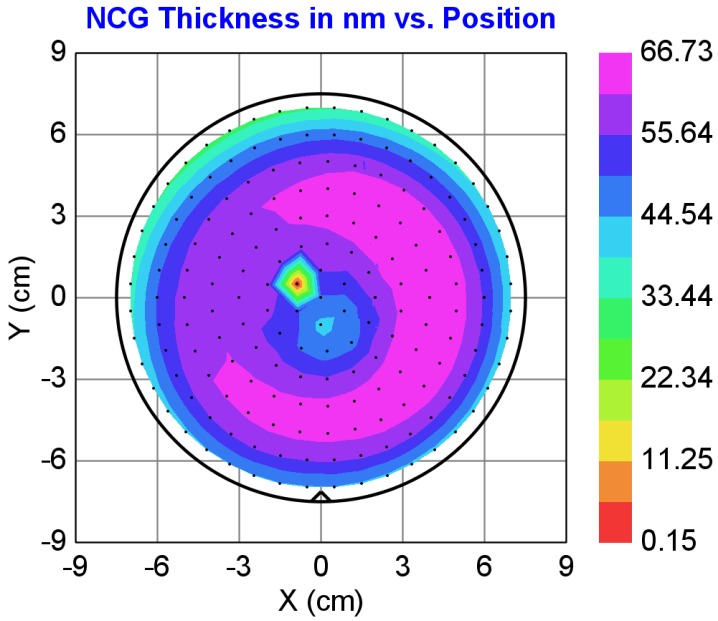

(d) $TSiO_2$ x13 (700 °C) with approximate NCG thickness between 44 nm to 66 nm.

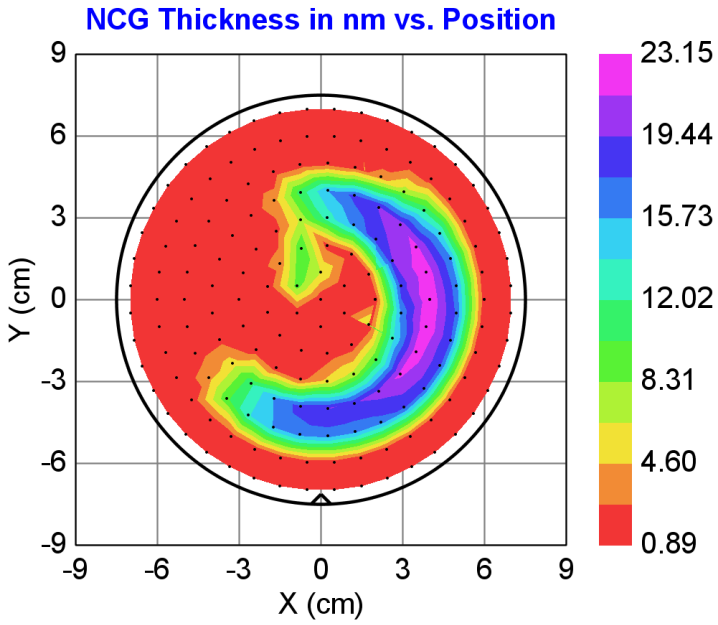

(e) $TSiO_2$ x14 (650 °C) with approximate NCG thickness between 0.8 nm to 23 nm.

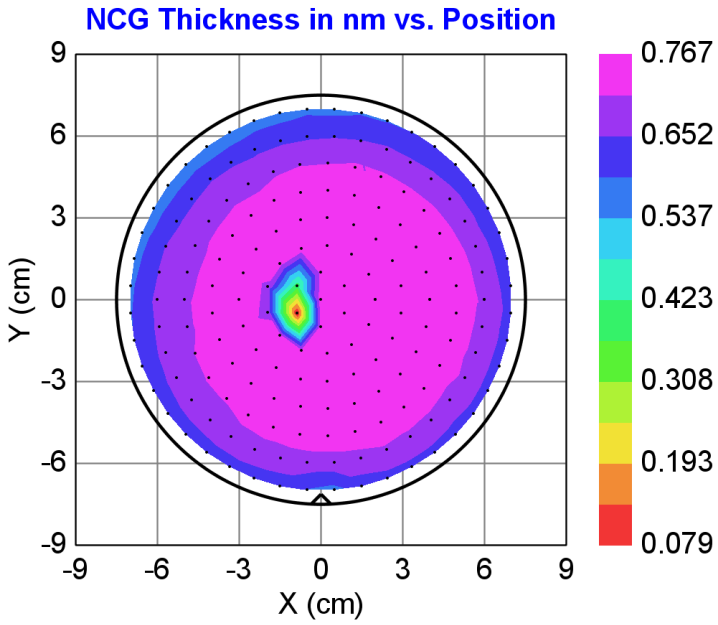

(f) $TSiO_2$ x15 (600 °C) with approximate NCG thickness between 0.6 nm to 0.7 nm

4.3.5 Discussion and Analysis

From **Figure 21**, it can be seen that there were non-uniformity of deposition of NCG film across the wafer in all deposition temperatures. This may be due to the temperature gradient effect on the wafer or due to plasma effect (plasma non-uniformity) in the chamber as a quartz sample was also positioned approximately in the middle part of the wafer used for optical transparency characterisation. This non-uniformity was not obvious when the deposition of NCG film was conducted without the present of quartz sample on the wafer.

From **Table 6**, it can be observed that the as-deposited NCG films were much *thicker* at high deposition temperatures with relatively low sheet resistance as compared to samples deposited at lower temperatures.

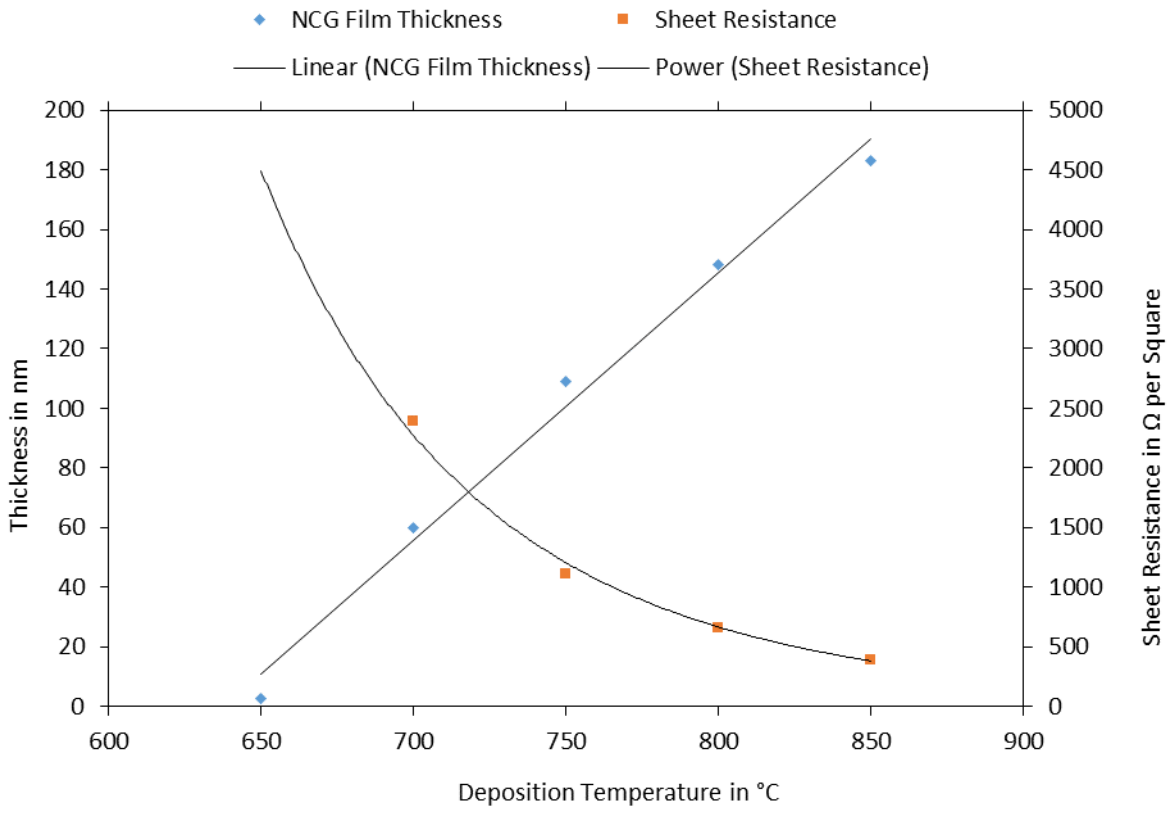

Figure 22. NCG film thickness and sheet resistance (using four-point probe) plots as a function of growth temperatures.

The resulting data for thickness was plotted and approximated using linear fit, whilst the sheet resistance data was plotted and forecasted up to 650 °C (as no measured data available) using power law function (**Figure 22**).

It can be seen that higher temperature produces thicker film with lower sheet resistance whilst lower deposition temperature yields thinner film with higher sheet resistance respectively. The measured NCG film thickness linear fitting plot follows closely to data points. With this linear relationship, theoretically a desired NCG thickness can be deposited at a particular temperature by tuning the deposition time while other deposition parameters remain unchanged. However, lowering deposition temperature below than 650 °C, does not mean that NCG film could be deposited by increasing deposition time. Further investigation needs to be conducted at what temperature or activation energy could decompose the CH_4 gas for NCG film to be deposited. Whilst the measured sheet resistance power law fitting follows closely the data points.

4.4 Deposition Rate and Activation Energy (E_a)

In this work, PECVD is used and the deposition of NCG films are exponentially temperature dependent and normally follows according to the Arrhenius equation[43] as shown below.

$$Rate, R = z(T).e\left(-\frac{E_a}{kT}\right) \qquad [43] \qquad \textbf{Equation 2}$$

Where Rate, R = Deposition rate

E_a = Activation Energy (eV)

k = Boltzmann constant (8.62×10^{-5} evK^{-1} or 1.38×10^{-23} JK^{-1})

T = Temperature in Kelvin (K)

z (T) = Pre-exponential factor

Using the deposition rates obtained from different growth temperatures activation energy, E_a can be extracted from the Arrhenius equation. E_a is the activation energy that the minimum energy molecules possess in order for a reaction to take place to form a product.

Taking the natural logarithm (Ln) of both sides of Equation 2 yields,

$$R = z(T).e\left(-\frac{E_a}{kT}\right)$$

$$\text{Ln R} = \text{Ln z(T)} - \left(\frac{\text{E}_\text{a}}{kT}\right) \qquad \text{rearranging}$$

$$\text{Ln R} = -\left(\frac{\text{E}_\text{a}}{kT}\right) + \text{Ln z(T)} \qquad \text{which has a form of a straight line equation, } y = mx + c$$

$$\text{where} \quad y = \text{Ln R} \qquad m = -\left(\frac{\text{E}_\text{a}}{k}\right) \qquad x = \frac{1}{\text{T}} \qquad c = \text{Ln z(T)}$$

A direct plot of R versus Deposition temperature will produce a curve that does not tell much story. However, plotting natural logarithm (Ln) R versus $\frac{1}{T(K)}$ or (K^{-1}) give a straight line. The data in Table 5 were plotted and fitted with linear fitting as shown in **Figure 23.**

Sample identifier	T_{dep} (°C)	Deposition rate (nm/min)	Ln Deposition Rate (nm/min)	1 / T_{dep} K^{-1}
$TSiO_2$ x 10	850	3.050	1.12	0.00089
$TSiO_2$ x 11	800	2.467	0.90	0.00093
$TSiO_2$ x 12	750	1.817	0.60	0.00098
$TSiO_2$ x 13	700	1.000	0.00	0.00103
$TSiO_2$ x 14	650	0.046	-3.08	0.00108

Table 7. Calculated natural logarithm (Ln) of deposition rate as a function of deposition temperature in K^{-1}. * Data for sample deposited at 600 °C was omitted due to no deposition took place.

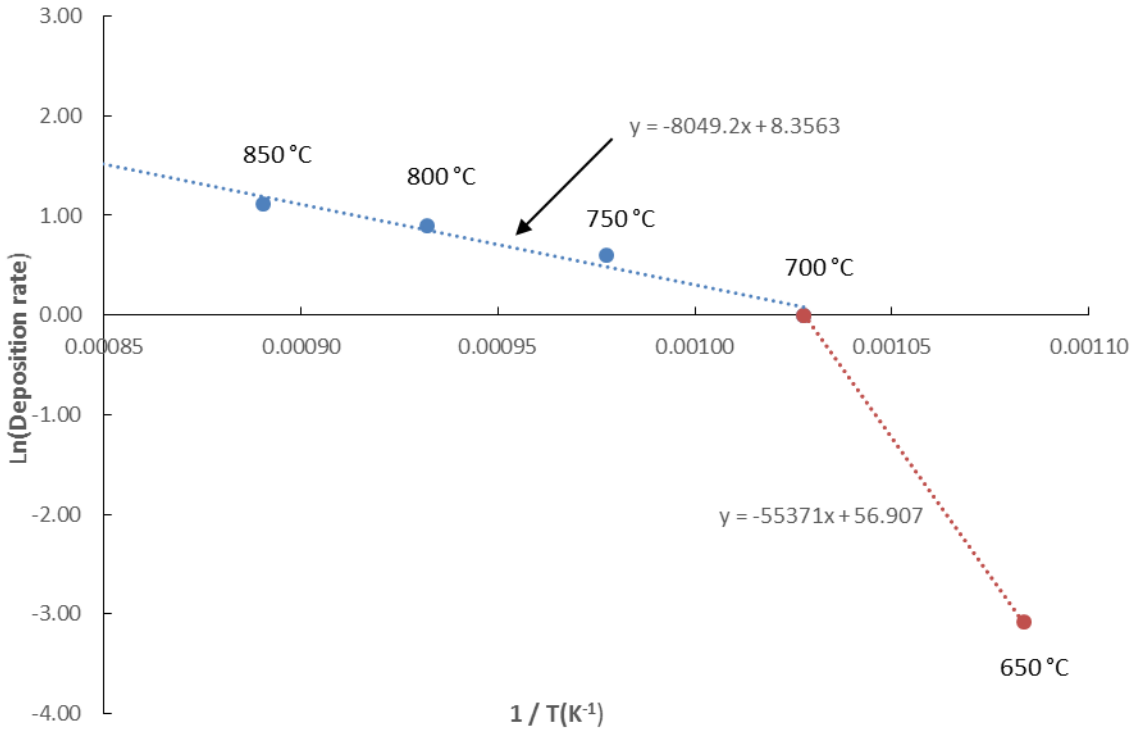

Figure 23. A graph plot of natural logarithm (Ln) of deposition rate as a function of deposition temperature in 1/T (K^{-1}).

From **Figure 23**, it can be observed that the plot has two slopes or regimes; high temperature regime between 700-850 °C and low temperature regime between 700-650 °C. These temperature regimes are common in most CVD reactions[43].

In high temperature regime, the slope is gradual; decreasing drastically in the low temperature regime. When temperature is low, the surface reaction is slow and an abundance of reactants is available. This reaction is termed surface reaction limited[43].

In the case of high temperature regime, the surface reaction increases exponentially and above a particular temperature all gas molecules react at the surface, hence thicker film deposition can be obtained. This reaction is termed mass transport regime (the deposition rate is dependent on the supply of new species to the surface.

The activation energy required in the mass transport limited is much lower than as required in surface reaction needed.

From the slope of the straight line in **Figure 23**, two values of E_a and z (T) can be derived:

High temperature regime

$$m = -\left(\frac{E_a}{k}\right) \qquad \text{rearranging}$$

$$E_a = -m_1.k = -(-8049.2) \times 8.62 \times 10^{-5}\ \frac{eV}{k} = 0.694\ eV$$

and

$$c = \text{Ln}\, z(T) = 8.3563 \qquad \text{hence,} \quad z(T) = e^{8.3563} = 4259.6$$

Low temperature regime

$$E_{a2} = -m_2.k = -(-55371) \times 8.62 \times 10^{-5}\ \frac{eV}{k} = 4.773\ eV$$

and

$$c = \text{Ln}\, z(T) = 56.907 \qquad \text{hence,} \quad z(T) = e^{56.907} = 5.18 \times 10^{24}$$

Having known the values for Ea and z (T), it can be seen that either by increasing the deposition temperature or decreasing the activation energy will yield in an increase in the deposition rate.

From the two derived E_as and compare them with the graph, the followings can be observed, that is, the reaction with higher E_a has a steeper slope (low deposition temperature); the slope is gradual with lower E_a.

4.5 Raman Spectroscopy of the NCG film

In this work, Raman spectroscopy was used to characterize the structural properties of the NCG film.

A Renishaw inVia Raman spectrometer with 532nm excitation wavelength, laser spot diameter of ~1 μm with 50 times magnification was used to characterize the NCG film deposited on the wafers. The tool was fitted with an automated xy sample stage with a range of approximately 70mm by 70 mm, hence limits a full wafer mapping. However, by carefully placing the wafer on the stage, several different points on the wafer were identified and characterised so that an optimum results of the Raman spectra of the deposited NCG film can be obtained.

4.5.1 Results and Analysis of Raman Spectroscopy of NCG film on SiO_2/Si Samples

The present of D (I_D), G (I_G) and 2D (I_{2D}) peaks [44] in all samples deposited at different temperatures exhibit that NCG film were deposited on the wafers. The Raman spectra of all samples shared similar characteristics with broad and overlap I_D and I_G peaks and low intensity of 2D peaks.

The high intensity of I_D peak at around 1350 cm^{-1}, indicates that the film has a large number of crystal defects or small domain size or nanocrystalline nature. Clearly, the present of this peak indicates that the NCG film was not a single layer graphene (SLG).

The I_G peak at around 1600 cm^{-1}, indicates that the film has sp^2 bonding of graphene properties. In SLG, the I_G peak is lower than I_{2D} peak. In this work, all I_G peaks are relatively higher that I_{2D} peaks which indicate that the deposited films were multilayers and very thick.

A relatively low I_{2D} peak that occurs around 2694 cm^{-1}, indicates the quality or crystalline nature and number of layer of graphene. Finally, the I_{D+G} peak which occurs around 2950 cm^{-1} indicates the graphitic disorder in the NCG film [45].

The Raman spectra of all samples as a function of different growth temperatures are shown in **Figure 24**(a), (b) and (c) respectively. All spectra except **Figure 24**(c) show similar characteristics with only differences in the intensity of the I_D, I_G and I_{2D} peaks respectively.

Figure 24(c) shows I_D and I_G peaks with very broad I_{2D} peaks, which is a characteristic of amorphous carbon.

The intensity ratio of I_D to I_G can be used as an indication of defect quantity: a low I_D / I_G corresponds to a small defect quantity. In addition, the ratio can be used to estimate the average domain size, L_a[12] (**Equation 1** on page 21) of the NCG film deposited at different temperatures and shown as in **Table 8.**

Sample identifier	T_{dep} (°C)	t_{dep} (Minute)	Thickness (nm)	(Four point probe) Sheet resistance ($\Omega.Sq^{-1}$)	Deposition rate (nm/min)	I_D / I_G	I_{2D} / I_G	Grain Size L_a (nm)
$TSiO_2$ x 10	850	60	183	394	3.03	1.703	0.259	2.9
$TSiO_2$ x 11	800	60	148	660	2.45	2.180	0.263	2.3
$TSiO_2$ x 12	750	60	109	1113	1.83	2.612	0.257	1.9
$TSiO_2$ x 13	700	60	60	2394	1.00	1.937	0.271	2.6
$TSiO_2$ x 14	650	60	2.75	undefined	0.05	1.467	0.141	3.4
$TSiO_2$ x 15	600	60	0.71	undefined	0.00	undefined	undefined	undefined

Table 8. Estimated average grain size, L_a as a function of deposition temperatures.

From **Table 8**, it can be observed that large grain size can be obtained at deposition temperature of 850 °C and the size reduced as the temperature decreases down to 750 °C. At temperatures lower than 750 °C, the grain size has increased again and largest at deposition temperature of 650 °C.

Also at 650 °C, the intensity of I_D to I_G ratio was at minimum exhibits a low density of grain boundaries but larger grain size. This characteristic may be because of better stacking order of graphene layer and carbon atoms bound each other 'properly' at this temperature. The sheet resistance of 650 °C sample was not obtainable due to the limitation of four-point probe for not being able to measure film thickness less than 50nm.

All except samples deposited at 600°C show relatively high intensity of I_{2D} to I_G ratio. The ratio intensity increases from 0.259 to 0.271 and this increase suggests that high presence of graphene even at 700 °C. The ratio of the I_{2D} to I_G can be used to estimate the number of graphene layer. In a pristine graphene, the intensity I_{2D} to I_G ratio is higher than 2 [47], which means that the intensity of 2D peak is much higher than the G peak. In this work, our I_{2D} to I_G ratio is relative low which indicates that the as-deposited NCG film is multi-layer graphene or rather graphite.

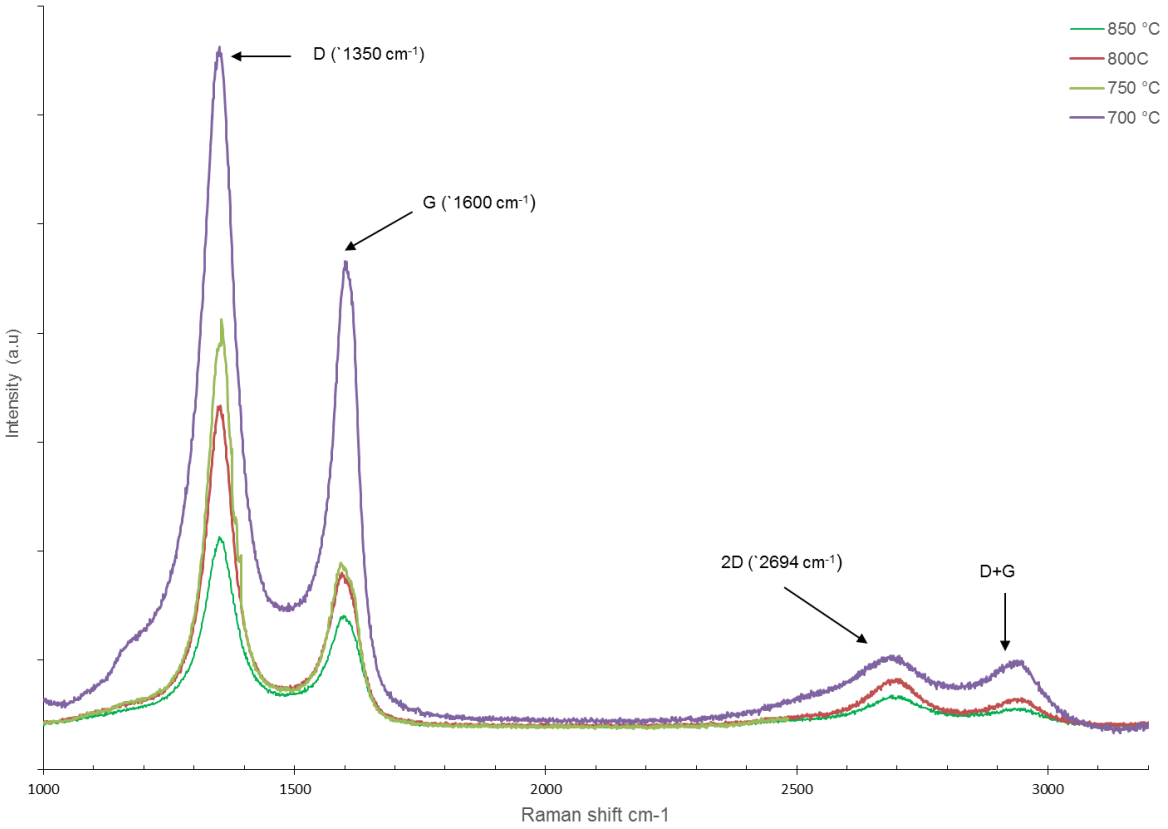

Figure 24. (a) Raman spectrum of NCG film deposited at different deposition temperatures.

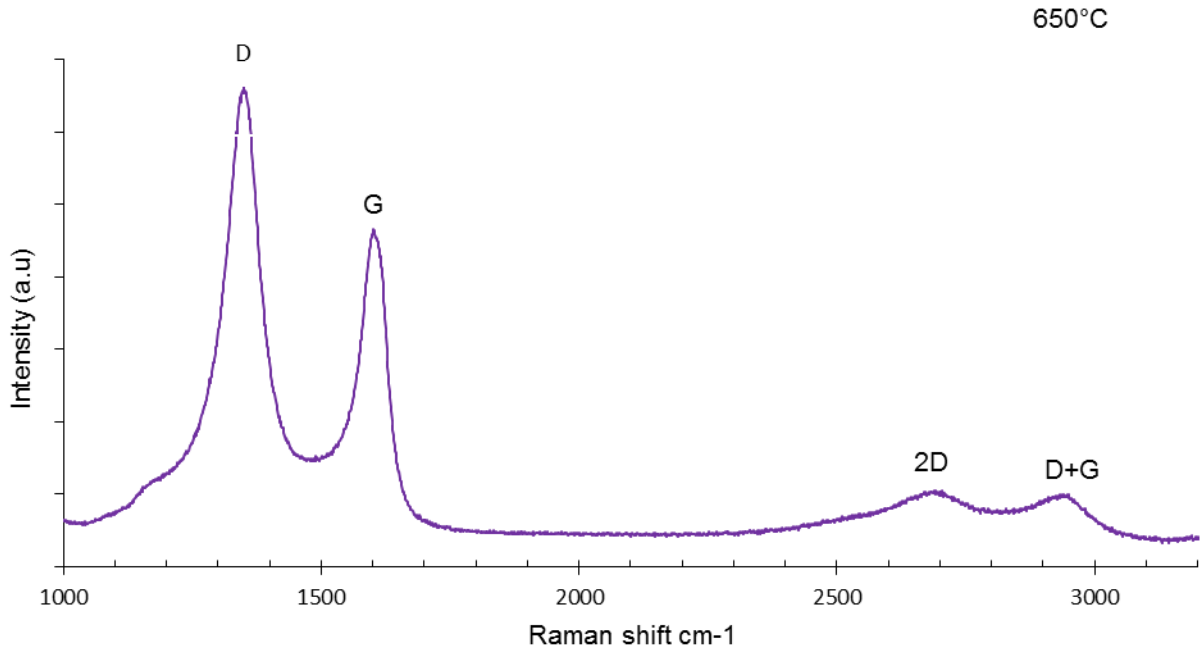

Figure 24. (b) Raman spectrum of NCG film deposited at 650 °C.

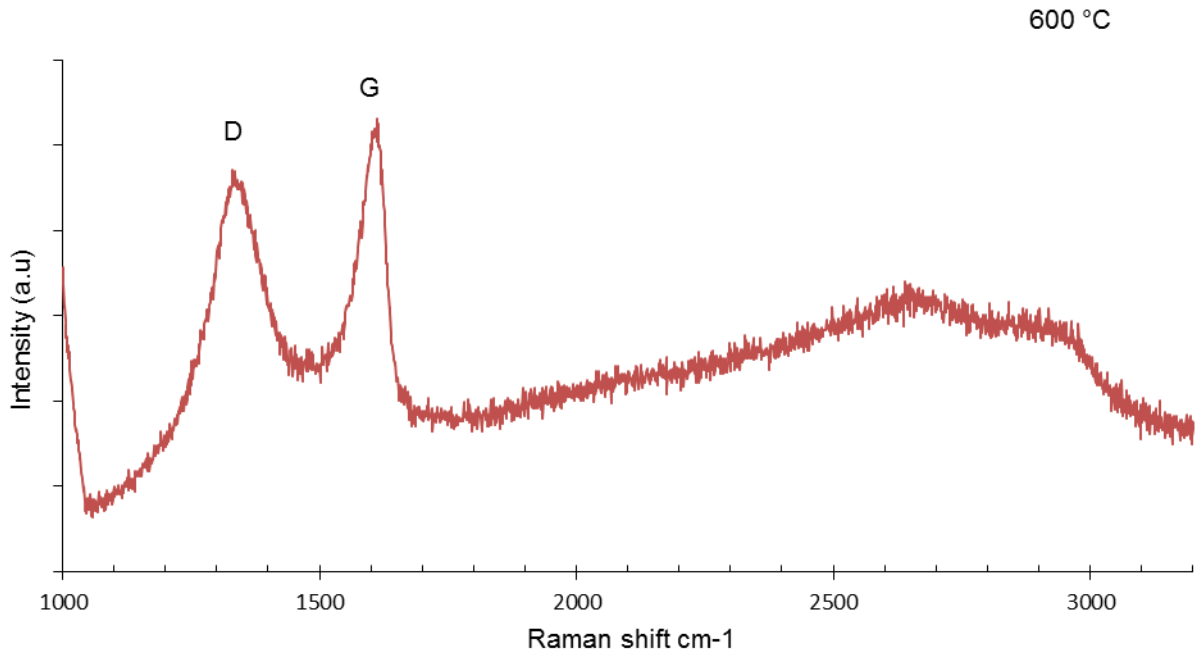

(c) Raman spectrum of NCG film deposited at 600 °C

4.5.2 Results and Analysis of Raman Spectroscopy of NCG film grown on Quartz samples

On each run of NCG deposition at different growth temperatures, a quartz sample of 10mm by 10mm, with 1 mm thickness was placed at the centre of the wafer. This was done to investigate the optical properties of the NCG film at different growth temperatures, keeping all deposition parameters and chamber condition unchanged.

No quartz samples deposited below 750 °C, show Raman spectra of NCG on the quartz, or in other words, no deposition took place. These results may be due to temperature gradient or low deposition temperature on the actual sample as it was placed on top of silicon wafer with 300 nm SiO_2, which acts as a poor thermal conductor. The actual temperature on the quartz probably much lesser than the set temperature which eventually limit surface reaction of the gas molecules on the quartz surface, and hence no deposition has occurred. Better deposition may be achieved by placing the quartz sample on a carrier wafer with good thermal conductivity such as a molybdenum wafer.

The Raman spectra of quartz samples deposited at 850 °C, 800 °C and 750 °C are similar as depicted in **Figure 24** (a) and (b), which has relatively high D and G peaks with low intensity of 2D peaks.

4.6 Conclusion

In this chapter, a deposition process has been developed in order to synthesis NCG film directly on SiO_2 substrate using RF-PECVD without metal catalyzed. In the first part of this work, only the growth temperatures were varied keeping other deposition parameters unchanged. The as-deposited NCG film on both Si/SiO_2 wafers and quartz samples was characterized and reported.

It was found that no NCG films were deposited on quartz samples at 750 °C and below. Although quartz samples deposited at higher than 750 °C Raman spectra of the NCG film can be observed but no optical transmittance reading was obtained which speculated incorrect apparatus set-up.

Further characterization of as-deposited NCG film on Si/SiO_2 substrate such as surface roughness measurement using AFM and sheet resistance using Hall measurement still yet need to be undertaken.

CHAPTER 5

Device Fabrication and Characterisations

This chapter explains the fabrication process of the deposited NCG film, and aims to characterize the electronic properties of the as deposited NCG film. A transmission line measurement (TLM) structure was used, as it was relatively simple method to measure the sheet resistance of a thin film material. Several transmission line method or measurement (TLM) and two-terminal device microstructures were fabricated based on the NCG film followed by metallization process of contacts pads using e-beam evaporator. These structures were used to investigate the properties such as the contact resistance and sheet resistance of the NCG film grown at temperature from 700 °C – 850 °C using Semiconductor parametric analyser tool.

In this work, the NCG film were deposited onto several n-doped single side polished 150 mm diameter silicon wafer with 300 nm wet thermally oxidized SiO_2. The NCG film deposition were carried out at different growth temperature while keeping other deposition parameters unchanged as shown in **Table 4.** on page 33. At every deposition temperature, a quartz sample of 10 mm x 10 mm of 1mm thickness was placed approximately in the middle part of the wafer sample for NCG film optical transparency and conductivity measurement purposes.

5.1 Fabrication Summary

An outline of the fabrication process of the TLM structures and devices are as follow:

All wafers marked as ($TSiO_2$ x10, $TSiO_2$ x11, $TSiO_2$ x12, $TSiO_2$ x13 and $TSiO_2$ x14) except wafer $TSiO_2$ x15, were used for device fabrication. The later was not process further due to very low uniformity coverage of NCG film, and this makes photolithography alignment challenging. Each sample having different thickness of NCG film, deposited at different growth temperatures were patterned into two different structures namely: a simple two-terminal devices and TLM structures.

First, the desired or patterned NCG film areas were isolated from the rest of the NCG on the wafer by photolithography. A positive resist was spun on top of the wafer in order to isolate the desired NCG by opening a rectangular strips that is,1805 µm x 300 µm and 50 µm x 20 µm for TLM and two terminal device respectively and subsequently reactive ion etching (RIE) the strips structure using anisotropic O_2 plasma etch. *The etching rate is approximately 25 nm/min. Hence, the RIE process for each wafer varies according to the NCG film thickness as shown in **Table 10**.

Then, metal contacts pads were aligned/exposed, and developed on the patterned NCG structures. Finally, a set of nickel / titanium (Ni / Ti) contacts were deposited by e-beam evaporation followed by lift-off process. Gold is commonly used as a thin layer to promote better adhesion to the under-laying material but it was expensive and unavailable at the time of metallization. Hence, titanium was an option. For the TLM structures, all Ni / Ti contacts have identical square of 200 μm^2. The separation between the pairs adjacent contacts were 30, 50, 75, 100 and 150 µm respectively.

In general, the complete fabrication process involved two optical lithography steps, one plasma etching of NCG film, and one e-beam evaporation of target metal for contacts pads. A more detail steps of the fabrication process are as outlined in **Table 9.**

NO	PROCESS	DESCRIPTION
1	**CLEANING**	Acetone/IPA
2	**LITHOGRAPHY 1**	Positive Resist - S1813 o Wafer dehydration > Oven @ 210 °C for 10 min o Spin Coating> thickness ~ 1 µm o Pre exposure bake > Hotplate @ 110 °C for 90 sec o Exposure > *Mask 1 o Development > Using MF319 for 45 sec o Rinse with water o Dry sample with N_2 air
3	**NCG RIE ETCHING**	Removal of unwanted NCG using O_2 plasma (generic O_2 etch recipe) o Gas flow and pressure > O_2 : 0 sccm and 30 mT o Plasma > RF power : 100 W o Etch rate and Time > approx. 20-25 nm/min and varies with NCG thickness
4	**RESIST STRIP**	Residual resist removal using Acetone/IPA
5	**LITHOGRAPHY 2**	Negative Resist – AZ2070 [i-line filter ON] o Wafer dehydration > Oven @ 210 °C for 10 min o Spin Coating > thickness ~ 4 µm o Pre exposure bake > Hotplate @ 115 °C for 90 sec o Exposure > *Mask 2, Alignment required on patterned NCG structure o Post exposure > Hotplate @ 115 °C for 70 sec o Development > Using AZ726 for 60 sec

	○ Rinse with water	
	○ Dry sample with N_2 air	
6	**METALIZATION**	Target metal Ti / Ni with thickness ratio of 10 / 50 nm
7	**LIFT-OFF PROCESS**	N-Methyl-2-Pyrrolidone (NMP)

Table 9. Detailed fabrication steps for both TLM and two terminal device structures.

Sample No	**NCG Thickness** (nm)	**Etching Time** (min)	**Etch rate (nm/min)**
$TSiO_2$ x10	160 - 200	8.5	25
$TSiO_2$ x11	125 - 150	7	25
$TSiO_2$ x12	80 - 113	5	25
$TSiO_2$ x13	44 - 66	5	25
$TSiO_2$ x14	8-23	4	25
$TSiO_2$ x15	0.9	2	25

Table 10. Different etching durations used in Step 3 for NCG structures fabrication.

The etching rate was derived from running a standard O_2 plasma RIE recipe on a known thickness of NCG film. The accuracy of the etching rate was confirmed by conducting several test run on sample wafers. Then, an ellisometer was used to verify if all the NCG was etched down to the SiO_2 layer. During the etching process, some thickness of the photoresist also etched away. Therefore, a proper thickness of the photoresist was spun onto the sample wafer so that it does not get etch and subsequently exposed the desired NCG film.

A microscope image of fabricated two-terminal device and TLM structures are shown in **Figure 26.** Figure 26(b), that is, TLM structures, a ‘crack’ like pattern can be seen. Initially, it was suspected that there were still some resist presence on it. After several acetone/IPA cleaning, the crack pattern can still be seen. Then, it may be due over contact/pressure between the mask and sample during exposure process. This was based on the finding that in the exposure recipe, the mask thickness was set to 3.5 mm, where it should have been set to 5 mm.

(a) Mask 1

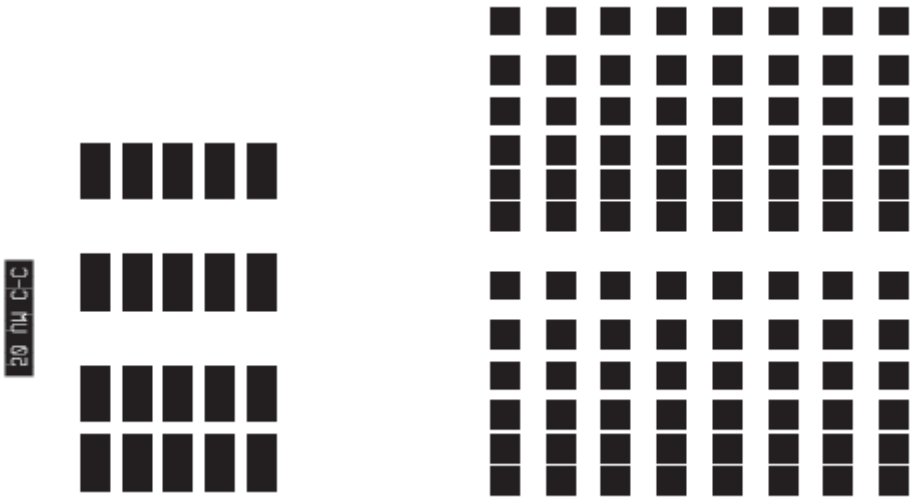

Two-Terminal device TLM structure

(b) Mask 2

Figure 25. Schematic illustration of the masks used for the fabricated structures. (a) Mask 1 – shows patterning bars/strips and rectangular shape, (b) Mask 2 - shows contact pads used on top of patterned NCG structures (Mask 1).

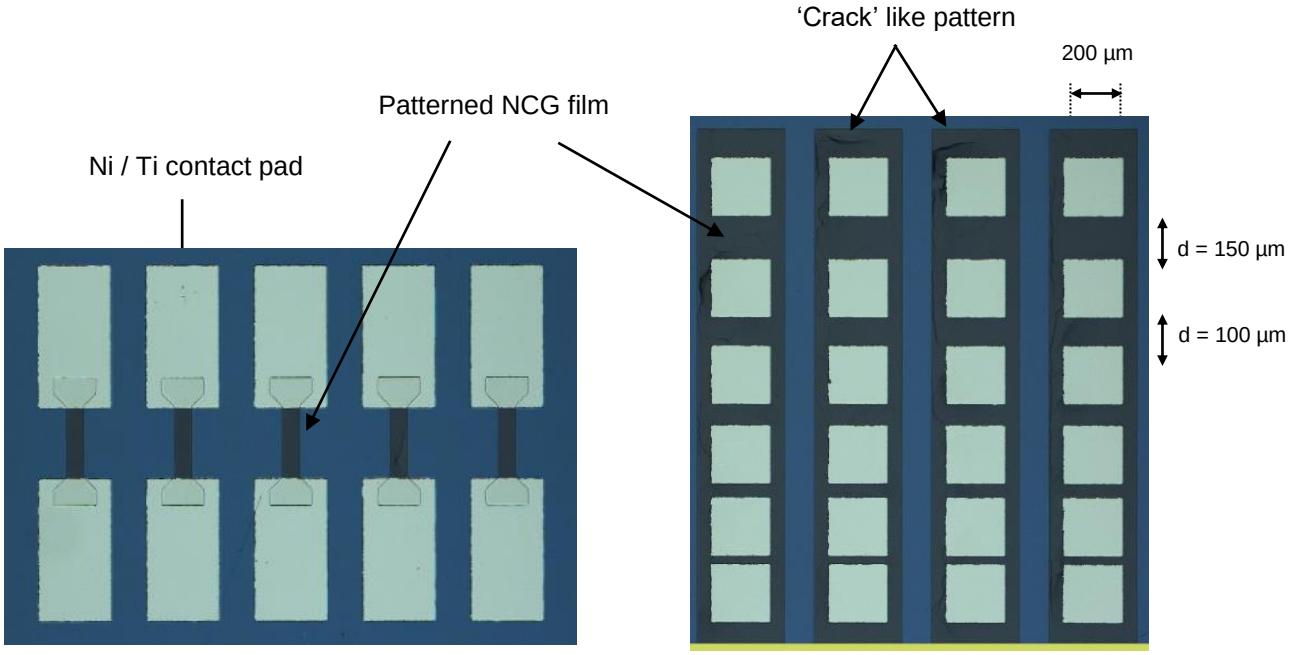

Figure 26. Optical images of fabricated (a) two terminal device and (b) TLM structures based on NCG film after metallization and lift-off processes.

5.2 Electrical Characterisation

The electronic transport properties of the patterned TLM structures were characterised by using a MEMS probe station and an Agilent B1500A semiconductor Device Analyser. A schematic representation of the fabricated NCG TLM structure and the measurement set-up was shown in **Figure 27.**

The TLM consists of a set of metal contact pads, that is, titanium/nickel (Ti/Ni) with identical geometry of length, L = 200 µm and width, W = 200 µm, with different spacing, d (30, 50, 75, 100 and 150 µm) between these contact pads and deposited onto a laterally isolated rectangular graphene area.

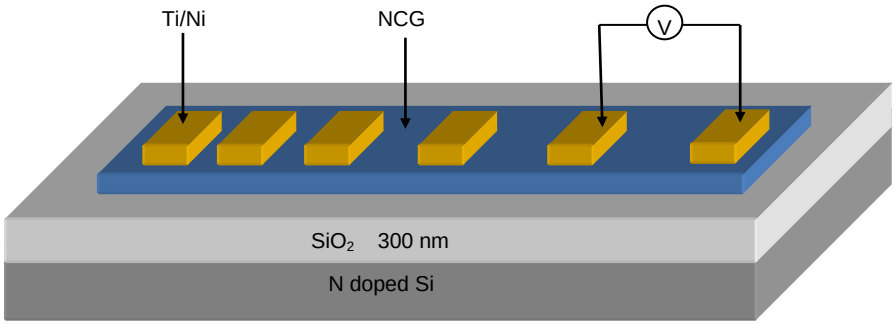

Figure 27. A schematic representation of the fabricated TLM structure with measurement setup. *V- Agilent B1500A semiconductor Device Analyser.

A voltage sweep (0-10V) was passed between two adjacent contacts through a pair of probes enabling current flow though the NCG film underneath the contacts. Hence, resistance between the pair of contacts can be obtained. The process was repeated for the rest of contact pairs and the total resistance was plotted as a function of metal contact pad spacing. The resultant current-voltage (I-V) characteristics for different distances between adjacent contacts for all samples were plotted as in **Figure 28.** Only two set of measurements were made on two separate TLM structures on each sample, with 6 contact pairs of different separation on each TLM structure.

5.3 Results

By linear fitting of the I-V curves for each sample, the resistance, R versus contact separation distance (d) curves can be obtained as shown in **Figure 28** (a) – (d). Once the resistance, R against contact separation distance curves have been plotted, the contact resistance, R_c and sheet resistance, R_{sh} of the NCG film can be derived using the **Equation 3** and the result as shown in **Table 11**.

From [46], the value of *R* can be defined as

$$R = 2R_c + \frac{R_{sh}}{W}.d \qquad \text{Equation 3}$$

Where R_c *is the resistance of the metal-NCG contact*
R_{sh} *is the NCG sheet resistance*
W is the width of the contact
d is the separation between contacts

The resistivity, ρ (Ω.cm) of the NCG film can also be determined if the thickness, *t* of the film is known and the relationship is given by

$$R_{sh} = \frac{\rho}{t} \qquad \text{Equation 4}$$

The reciprocal of ρ, gives the conductivity (σ) of a material in interest. This value is a measure of a material's ability to conduct electric current. The unit is siemens (S) per cm.

5.3.1 Sample Calculation

For an example, as obtained from **Figure 28**(a), and by linear fitting, the curve has an equation

$$1.6074x + 56.59 \qquad \text{Equation 5}$$

Let an equation of a straight line is **y = mx +c** Equation 6

Where m = slope or gradient of the line
x = x-axis intercept
c = y-intercept

Comparing Equation 3, Equation 5 and Equation 6 gives

$$\text{Slope m} = \frac{R_{sh}}{W} = 1.6074$$

$$R_{sh} = 1.6074 \times W \qquad \textit{where } W = 200\ \mu m$$

Hence $R_{sh} = \mathbf{\underline{321\ \Omega.sq^{-1}}}$

and

$$C = 2R_c = 56.59$$

$$R_c = \mathbf{\underline{28\ \Omega}}$$

Using Equation 4 to determine resistivity, ρ and since the thickness, *t* of the NCG film is known, that is 183 nm.

$$\text{Then, } \rho = R_{sh} \times t$$

$$= 321 \times (183 \times 10^{-9}) / (1 \times 10^{-2})$$

$$= \mathbf{\underline{5.87\ m\Omega.cm}}$$

Other calculated sheet resistance, resistivity and contact resistance of the NCG film deposited at different temperatures is shown in **Table 9.**

*No reading can be obtained from sample deposited at 650 °C due to very thin or no deposition of NCG film.

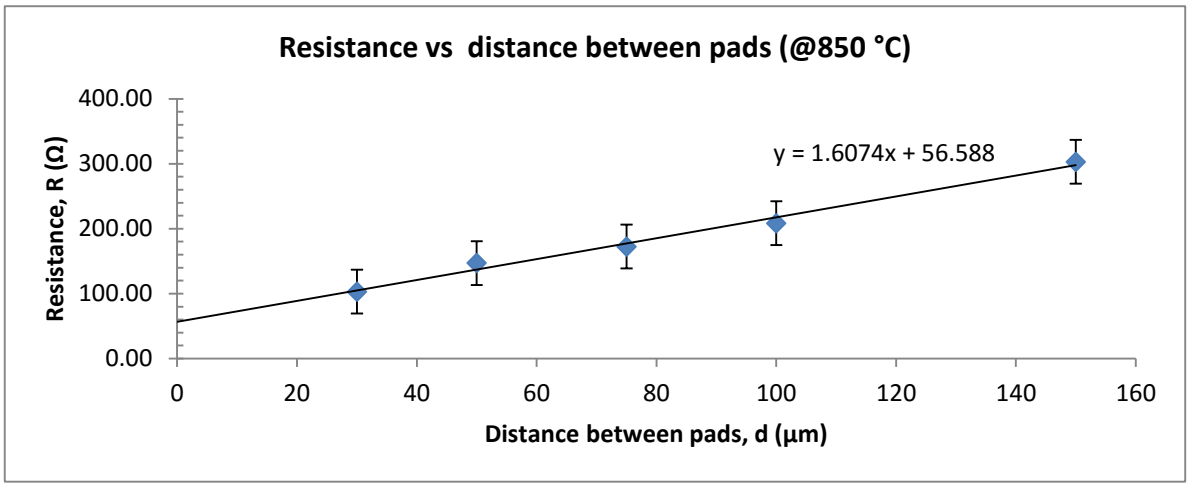

(a) at 850 °C

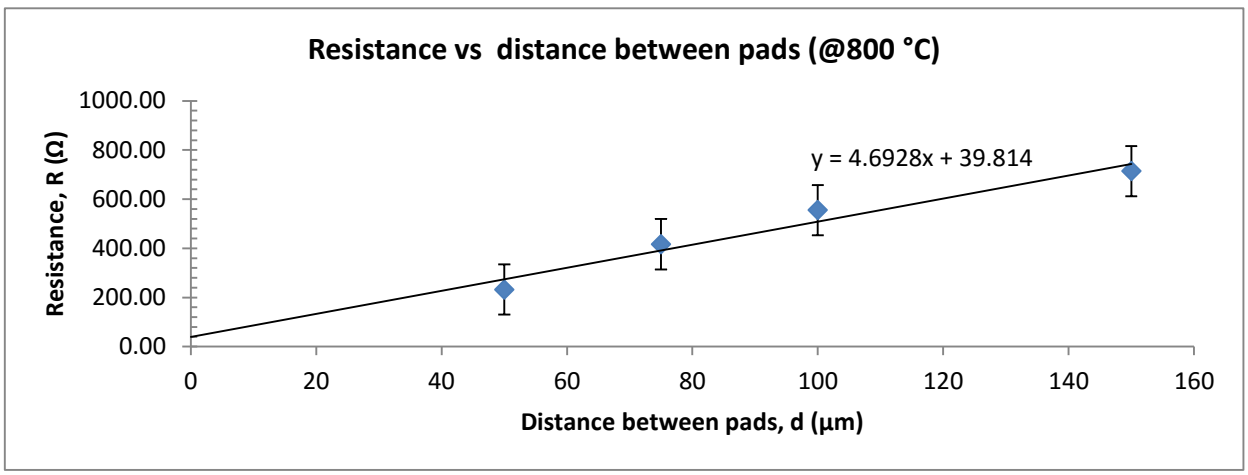

(b) at 800 °C

Figure 28. (a)-(d). The Resistance, *R* versus separation *d* between pair of contacts for TLM structures at different growth temperatures.

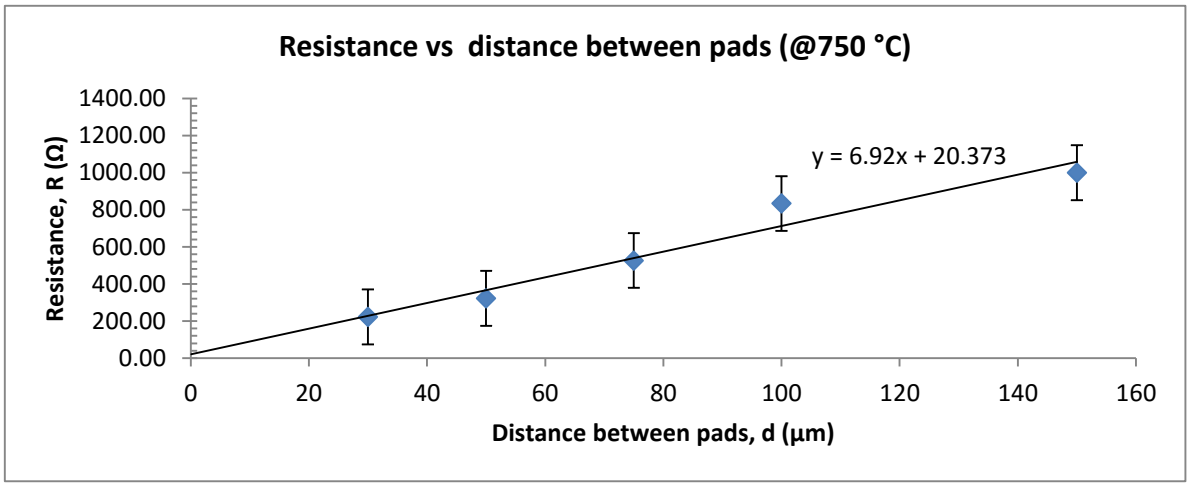

(c) at 750 °C

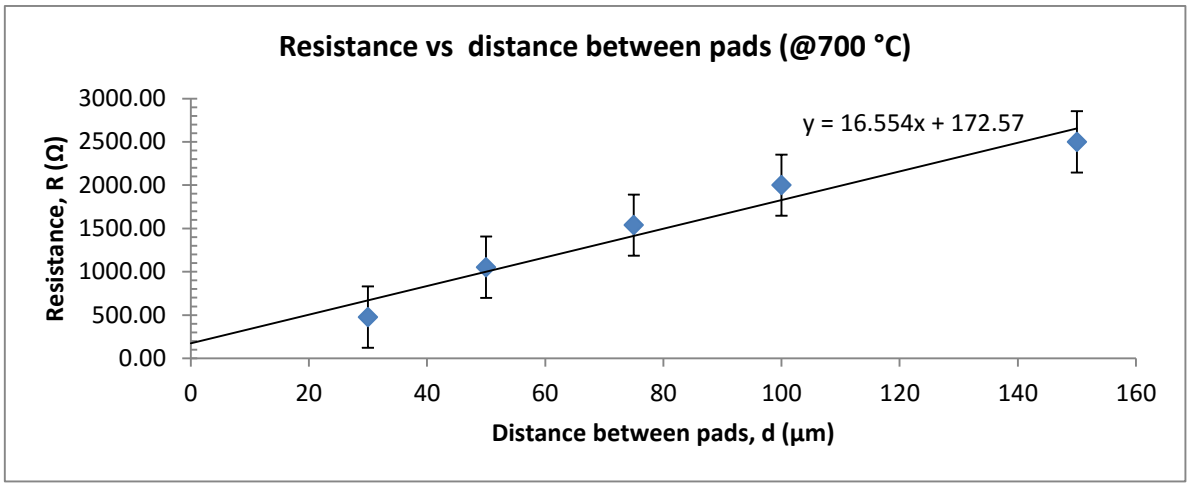

(d) at 700 °C

Figure 28. Cont. (a)-(d). The Resistance, *R* versus separation *d* between pair of contacts for TLM structures at different growth temperatures

5.4 Discussion and Analysis

The sheet resistance and resistivity results obtained from four-point probe and TLM structures techniques are compared as in **Table 11**.

Sample identifier	T_{dep} (°C)	Thickness, t (nm)	Four point Probe measurement		TLM structure measurement			Difference in R_{sh} & p between two measurement techniques (%)
			Sheet Resistance, R_{sh} ($\Omega.Sq^{-1}$)	Sheet resistivity, p (mΩ.cm)	Sheet Resistance, R_{sh} ($\Omega.Sq^{-1}$)	Sheet resistivity, p (mΩ.cm)	Contact Resistance (Ω)	
$TSiO_2$ x 10	850	183	394	7.2	321	5.9	28	18.53
$TSiO_2$ x 11	800	148	660	9.8	934	13.8	20	41.52
$TSiO_2$ x 12	750	109	1113	12.1	1384	15.1	10	24.35
$TSiO_2$ x 13	700	60	2395	14.4	3310	19.9	86	38.20
$TSiO_2$ x 14	650	2.75	undefined	undefined	undefined	undefined	undefined	undefined
$TSiO_2$ x 15	600	0.71	undefined	undefined	undefined	undefined	undefined	undefined

Table 11. Comparison of the derived contact resistance, sheet resistance and resistivity of NCG film using TLM structures technique and four-point probe measurement. *For Sample marked Wafer $TSiO_2$ x 14 and $TSiO_2$ x 15, no result were made available due to very low deposition of NCG film on the wafer side where the TLM structures were fabricated.

The average Resistance, *R* versus separation *d* between pair of contacts for TLM structures at different growth temperatures results obtained for the 4 samples are shown in **Figure 28(a)-(d)**. From the two set of measurements of each TLM structure on each deposition temperature, the measured data has an average uncertainty of points by 5% (error bars).

The obtained data were plotted - the NCG film thickness versus deposition temperature was approximated using a linear fit (10% error) and a power law function fit (5% error) for sheet resistance graph versus temperatures respectively. Both these fits matched closely to the data points (**Figure 29**). It can be seen that the sheet resistance R_{sh} decreased as NCG film thickness increased with an increase of deposition temperature. The graph is similar to the result obtained using four-point probe, in which thicker film with decreasing R_{sh} as temperature increased.

Resistivity, p is an intrinsic property of material which opposes the flow of current. A thicker NCG films deposited at high temperatures shows a low resistivity that allows easy flow of current in the material. **Figure 30.** shows that an increased in NCC film thickness resulting a reduction of the film resistivity and subsequently, an increase in the mobility of the carrier. The sheet resistivity graph is slightly offset from the actual data point (15% error), which may be due to the different thickness of the underlying NCG film.

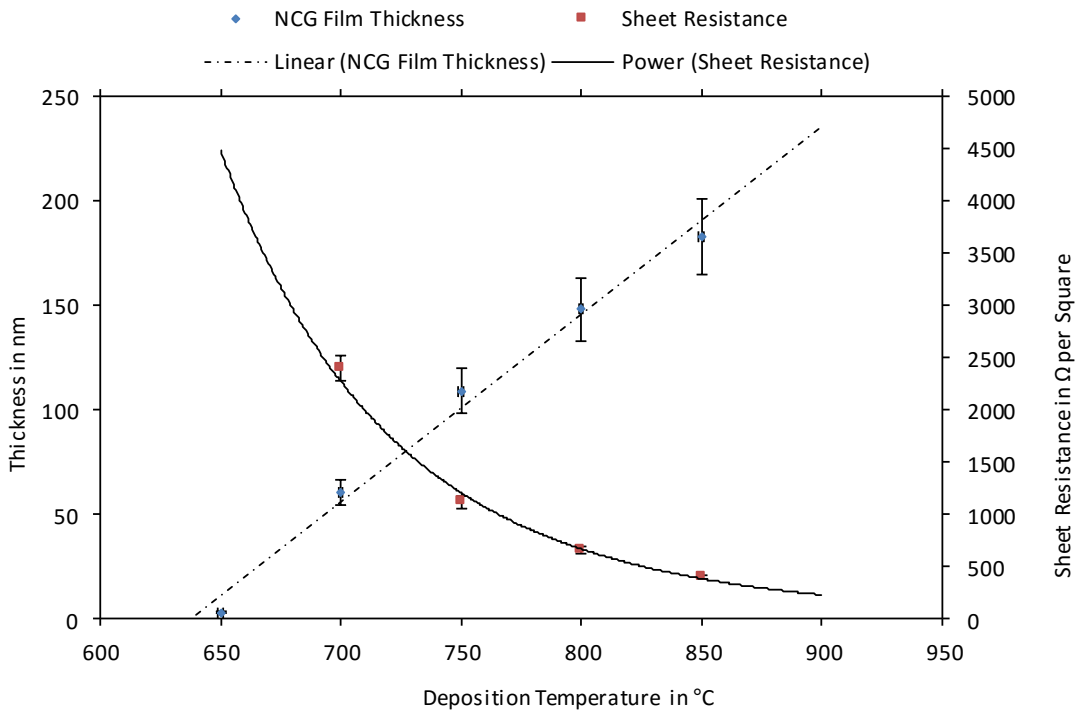

Figure 29. NCG film thickness and sheet resistance plots as a function of growth temperature, as measured by TLM technique.

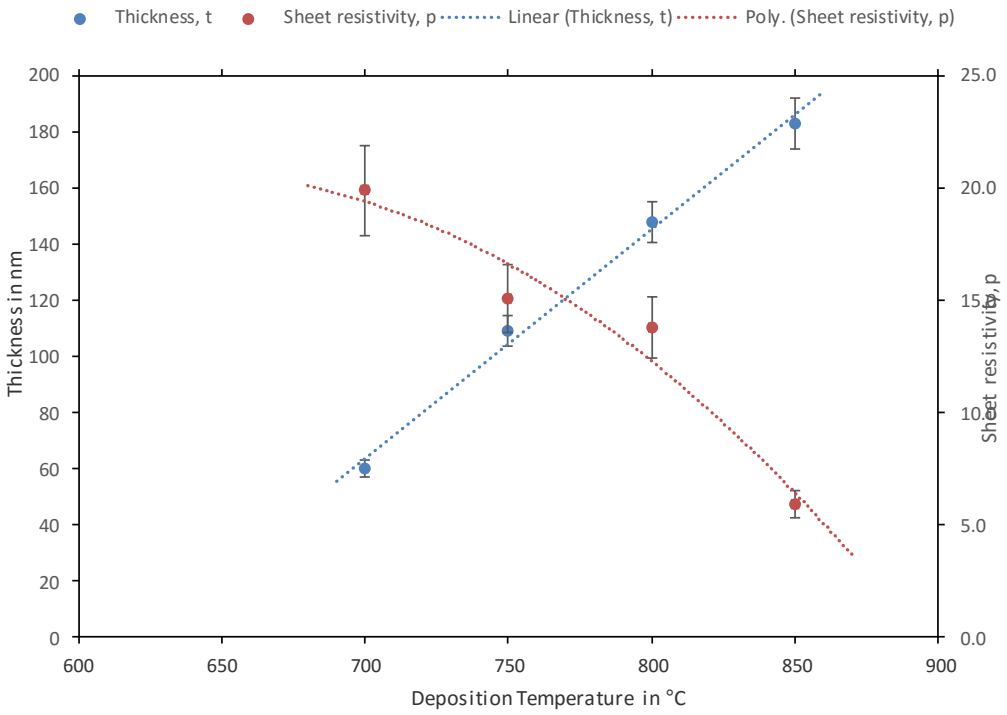

Figure 30. NCG film thickness and resistivity plots as a function of growth temperature, as measured by TLM technique.

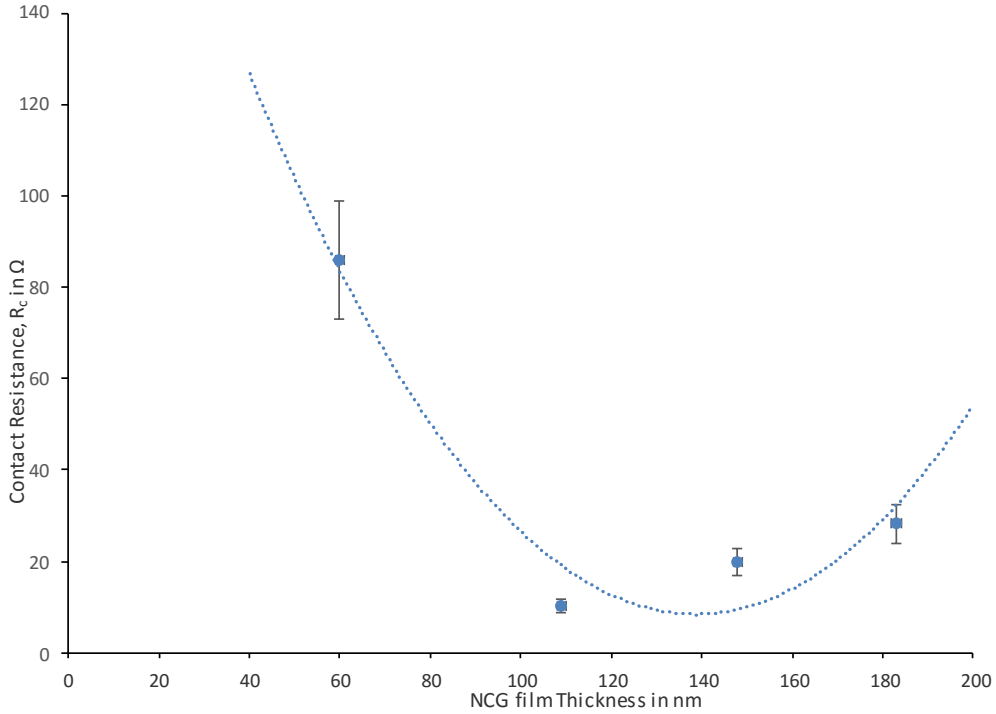

Figure 31. Contact resistance, R_c as a function of NCG film thickness

Figure 31 shows a contact resistance, R_c, versus the NCG film thickness, *t.* The data was approximated plotted using a polynomial fit (15% error) with only two data points on the curve. The calculated R_c derived from TLM technique indicates that the value reduces from 28Ω to 10Ω at temperature range of 850 °C to 750 °C respectively. It is observed that R_c is not uniform on different NCG film thickness; lower value of R_c at thin film (750 °C) which probably due to good adhesion between metal contact and underlying NCG film as compared to high R_c at thicker (850 °C) underlying NCG film. At 700 °C, the R_c is 86 Ω, which is relatively high due to poor adhesion between metal contacts and underlying NCG film, which is thinner than those deposited at higher than 700 °C. Undefined values of R_c at temperature range of 600-650 °C may be due to no NCG film being deposited on the SiO_2 wafer, hence no metal contact deposited on the sample wafer.

5.4.1 Comparison of R_{sh} and *p* values between the two measurements techniques

The differences in resistance and resistivity values between the two measurement techniques are between 18-42 %. A relatively high difference between the two values may be due to the simplicity of four-point probe technique resulting a poor set of data obtained. Although TLM technique gives, more reading that is accurate but additional fabrication steps involved have also introduced contamination or deterioration on the NCG film. As in a four-point probe measurement, no contact resistance measurement was made available.

5.5 Conclusion

In conclusion, TLM and two terminal device structures were fabricated successfully. Using TLM structures the electrical properties of the NCG films such as sheet resistance and contact resistance can be derived. Two terminal device characterisation is yet to be investigated.

Further work needs to be done at growth deposition temperature of 650 °C as the structures cannot be fabricated due to no or little deposition took place with quartz placed on top of wafer.

.

.

CHAPTER 6

Conclusions and Future Work

6.1 Conclusions

In this report, a deposition process has been successfully developed for synthesize of NCG film directly on a full size of 150 mm on Si/SiO_2 substrate, without metal catalyst using RF-PECVD. This work is considered as a novel approach whereby NCG film can be reproducibly fabricated at temperature as low as 650 °C without metal catalyst. This method avoids expensive and complicated post transfer process of the NCG film and compatible with current fabrication technologies

Although the quality of the as-deposited film is not yet as good as pristine graphene or thermal CVD grown graphene but continuous optimization of the deposition process or through doping technique would be possible to optimize the quality of the film suitable for applications such as a transparent conductive electrodes.

In this work, the best sheet resistance, R_{sh} as measured using four point probe and TLM measurement is 394 $\Omega.Sq^{-1}$ and 321 $\Omega.Sq^{-1}$ respectively for NCG sample deposited at 850° C with a thickness of 183 nm and sheet resistivity of 5.9 mΩ.cm. The R_{sh} deposited in the range of 700-850 °C are generally lower than those in the literature presented in Table 2. but this may be due to the as-deposited NCG film being thicker. With thicker film, obviously optical absorption is very high. An optical transmittance characterization was conducted on quartz sample deposited at various temperature but no valid result can be obtained probably due to the apparatus setting issue. The presence of Raman spectra can be observed at both samples on SiO_2 and quartz deposited between 650-850 °C and 750-850 °C respectively, with high D peak, low G peak and broad 2D peak indicates the film is nanocrystalline with high defect and multilayer graphene. The grain size of the NCG film is between 1.8-3.3 nm.

It is observed that deposition of the NCG film across the whole wafer is not uniform. This is due to the inclusion of a small (10x10 mm) quartz sample on the full wafer which was positioned close to the center of the wafer during deposition process. Better uniformity is achieved when there was only one wafer in the chamber during deposition took place.

In comparison with other film reported in Table 2, left alone ITO, currently our film is not competitive as yet and unsuitable for transparent conducting electrode but may be useful for other applications. In this work, the NCG film can be deposited at temperature as low as 650 °C, which is relatively lower than most deposition temperature as reported in Table 2 with lower sheet resistance, although being thicker but further tuning of deposition parameters may improve the quality of the NCG film.

6.2 Future work

The following points are highlighted for further works and investigations:

- To repeat the deposition of NCG film on quartz place directly on top of molybdenum carrier wafer. In this work, all quartz sample of 10 mm x 10 mm of 1mm thickness were placed on top of silicon wafer with 300 nm SiO_2, which acts as a poor thermal conductor. The actual temperature on the quartz probably much lesser than the set temperature, which eventually limit surface reaction of the gas molecules on the quartz surface. It is believe that by placing the quartz sample on a carrier wafer with good thermal conductivity such as a molybdenum wafer, better deposition can be achieved.

- Optical transmittance characterization of NCG film grown directly on quartz samples. Although the Raman spectrum of as-deposited NCG film grown at 750-850 °C in previous work can be observed but optical transmittance characterization has been unsuccessful. This may be due to improper set up of the transmittance apparatus.

- To further characterize the as deposited NCG film on Si/SiO_2 wafers in particular surface roughness and grain size characterization using AFM and sheet resistance using Hall

As mentioned earlier the NCG film properties such as sheet resistance, in this work is still far behind from the quality of metal catalyst graphene and not even close to the ITO quality, but more work can be done to improve the quality of the film. Amongst many strategies that can be explored further on how to improve the quality of the film so that it is suitable for at least transparent conductor application would be as outlined below:

- Improving the NCG grain size and boundaries by further optimising the synthesizing process such as tuning deposition parameters like, growth time, mixtures or flow rate of gases, pressure, etc.;
- Improving topography of the film such as minimising its surface roughness as this reducing the performance of the materials by limiting the charge transport (electron mean free path);
- Using doping technique by adding conductive material such as nitrogen or boron as these semiconductors will increase carrier densities.

REFERENCES

[1] A. K. Geim and K. S. Novoselov, "The rise of graphene," *Nat Mater,* vol. 6, pp. 183-191, Mar 2007.

[2] Y. Lee and J. H. Ahn, "Graphene-Based Transparent Conductive Films," *Nano,* vol. 8, Jun 2013.

[3] K. S. Novoselov, A. K. Geim, S. V. Morozov, D. Jiang, Y. Zhang, S. V. Dubonos, I. V. Grigorieva, and A. A. Firsov, "Electric field effect in atomically thin carbon films," *Science,* vol. 306, pp. 666-669, Oct 22 2004.

[4] K. S. Novoselov, D. Jiang, F. Schedin, T. J. Booth, V. V. Khotkevich, S. V. Morozov, and A. K. Geim, "Two-dimensional atomic crystals," *Proc Natl Acad Sci U S A,* vol. 102, pp. 10451-10453, Jul 26 2005.

[5] K. V. Emtsev, A. Bostwick, K. Horn, J. Jobst, G. L. Kellogg, L. Ley, J. L. McChesney, T. Ohta, S. A. Reshanov, J. Rohrl, E. Rotenberg, A. K. Schmid, D. Waldmann, H. B. Weber, and T. Seyller, "Towards wafer-size graphene layers by atmospheric pressure graphitization of silicon carbide," *Nat Mater,* vol. 8, pp. 203-207, Mar 2009.

[6] C. Berger, Z. M. Song, T. B. Li, X. B. Li, A. Y. Ogbazghi, R. Feng, Z. T. Dai, A. N. Marchenkov, E. H. Conrad, P. N. First, and W. A. de Heer, "Ultrathin epitaxial graphite: 2D electron gas properties and a route toward graphene-based nanoelectronics," *Journal of Physical Chemistry B,* vol. 108, pp. 19912-19916, Dec 30 2004.

[7] X. Z. Yu, C. G. Hwang, C. M. Jozwiak, A. Kohl, A. K. Schmid, and A. Lanzara, "New synthesis method for the growth of epitaxial graphene," *Journal of Electron Spectroscopy and Related Phenomena,* vol. 184, pp. 100-106, Apr 2011.

[8] A. Reina, X. Jia, J. Ho, D. Nezich, H. Son, V. Bulovic, M. S. Dresselhaus, and J. Kong, "Large area, few-layer graphene films on arbitrary substrates by chemical vapor deposition," *Nano Lett,* vol. 9, pp. 30-5, Jan 2009.

[9] X. S. Li, W. W. Cai, J. H. An, S. Kim, J. Nah, D. X. Yang, R. Piner, A. Velamakanni, I. Jung, E. Tutuc, S. K. Banerjee, L. Colombo, and R. S. Ruoff, "Large-Area Synthesis of High-Quality and Uniform Graphene Films on Copper Foils," *Science,* vol. 324, pp. 1312-1314, Jun 5 2009.

[10] S. Bae, H. Kim, Y. Lee, X. F. Xu, J. S. Park, Y. Zheng, J. Balakrishnan, T. Lei, H. R. Kim, Y. I. Song, Y. J. Kim, K. S. Kim, B. Ozyilmaz, J. H. Ahn, B. H. Hong, and S. Iijima, "Roll-to-roll production of 30-inch graphene films for transparent electrodes," *Nat Nanotechnol,* vol. 5, pp. 574-578, Aug 2010.

[11] A. Reina, S. Thiele, X. T. Jia, S. Bhaviripudi, M. S. Dresselhaus, J. A. Schaefer, and J. Kong, "Growth of Large-Area Single- and Bi-Layer Graphene by Controlled Carbon Precipitation on Polycrystalline Ni Surfaces," *Nano Research,* vol. 2, pp. 509-516, Jun 2009.

[12] H. Medina, Y. C. Lin, C. H. Jin, C. C. Lu, C. H. Yeh, K. P. Huang, K. Suenaga, J. Robertson, and P. W. Chiu, "Metal-Free Growth of Nanographene on Silicon Oxides for Transparent Conducting Applications," *Advanced Functional Materials,* vol. 22, pp. 2123-2128, May 23 2012.

[13] J. Y. Chen, Y. G. Wen, Y. L. Guo, B. Wu, L. P. Huang, Y. Z. Xue, D. C. Geng, D. Wang, G. Yu, and Y. Q. Liu, "Oxygen-Aided Synthesis of Polycrystalline Graphene on Silicon Dioxide Substrates," *Journal of the American Chemical Society,* vol. 133, pp. 17548-17551, Nov 9 2011.

[14] J. Sun, M. T. Cole, N. Lindvall, K. B. K. Teo, and A. Yurgens, "Noncatalytic chemical vapor deposition of graphene on high-temperature substrates for transparent electrodes," *Applied Physics Letters,* vol. 100, Jan 9 2012.

[15] L. C. Zhang, Z. W. Shi, Y. Wang, R. Yang, D. X. Shi, and G. Y. Zhang, "Catalyst-free growth of nanographene films on various substrates," *Nano Research,* vol. 4, pp. 315-321, Mar 2011.

[16] A. Ismach, C. Druzgalski, S. Penwell, A. Schwartzberg, M. Zheng, A. Javey, J. Bokor, and Y. G. Zhang, "Direct Chemical Vapor Deposition of Graphene on Dielectric Surfaces," *Nano Lett,* vol. 10, pp. 1542-1548, May 2010.

[17] S. K. Jerng, D. S. Yu, Y. S. Kim, J. Ryou, S. Hong, C. Kim, S. Yoon, D. K. Efetov, P. Kim, and S. H. Chun, "Nanocrystalline Graphite Growth on Sapphire by Carbon Molecular Beam Epitaxy," *Journal of Physical Chemistry C,* vol. 115, pp. 4491-4494, Mar 24 2011.

[18] http://en.wikipedia.org/wiki/Allotropes_of_carbon.

[19] J. Hass, W. A. de Heer, and E. H. Conrad, "The growth and morphology of epitaxial multilayer graphene," *Journal of Physics: Condensed Matter,* vol. 20, p. 323202, 2008.

[20] Z. H. Ni, H. M. Wang, J. Kasim, H. M. Fan, T. Yu, Y. H. Wu, Y. P. Feng, and Z. X. Shen, "Graphene thickness determination using reflection and contrast spectroscopy," *Nano Lett,* vol. 7, pp. 2758-2763, Sep 2007.

[21] N. Savage, "Graphene Makes Transistors Tunable," *Ieee Spectrum,* vol. 46, pp. 20-20, Sep 2009.

[22] C. N. R. Rao, K. S. Subrahmanyam, H. S. S. R. Matte, B. Abdulhakeem, A. Govindaraj, B. Das, P. Kumar, A. Ghosh, and D. J. Late, "A study of the synthetic methods and properties of graphenes," *Science and Technology of Advanced Materials,* vol. 11, Oct 2010.

[23] K. S. Kim, Y. Zhao, H. Jang, S. Y. Lee, J. M. Kim, K. S. Kim, J. H. Ahn, P. Kim, J. Y. Choi, and B. H. Hong, "Large-scale pattern growth of graphene films for stretchable transparent electrodes," *Nature,* vol. 457, pp. 706-710, Feb 5 2009.

[24] C. N. R. Rao, K. Biswas, K. S. Subrahmanyam, and A. Govindaraj, "Graphene, the new nanocarbon," *Journal of Materials Chemistry,* vol. 19, pp. 2457-2469, 2009.

[25] Z. S. Claire Berger, Tianbo Li, Xuebin Li, Asmerom Y. Ogbazghi, Rui Feng,, A. N. M. Zhenting Dai, Edward H. Conrad, Phillip N. First, and, and W. A. d. Heer*, "Ultrathin Epitaxial Graphite 2D Electron Gas Properties and a Route toward Graphene-based Nanoelectronics."

[26] S. Lee, K. Lee, and Z. H. Zhong, "Wafer Scale Homogeneous Bilayer Graphene Films by Chemical Vapor Deposition," *Nano Lett,* vol. 10, pp. 4702-4707, Nov 2010.

[27] W. Yang, C. L. He, L. C. Zhang, Y. Wang, Z. W. Shi, M. Cheng, G. B. Xie, D. M. Wang, R. Yang, D. X. Shi, and G. Y. Zhang, "Growth, Characterization, and Properties of Nanographene," *Small,* vol. 8, pp. 1429-1435, May 7 2012.

[28] J. Sun, N. Lindvall, M. T. Cole, T. Wang, T. J. Booth, P. Boggild, K. B. K. Teo, J. Liu, and A. Yurgens, "Controllable chemical vapor deposition of large area uniform nanocrystalline graphene directly on silicon dioxide," *Journal of Applied Physics,* vol. 111, Feb 15 2012.

[29] J. Sun, N. Lindvall, M. T. Cole, K. B. K. Teo, and A. Yurgens, "Large-area uniform graphene-like thin films grown by chemical vapor deposition directly on silicon nitride," *Applied Physics Letters,* vol. 98, Jun 20 2011.

[30] M. H. Rummeli, A. Bachmatiuk, A. Scott, F. Borrnert, J. H. Warner, V. Hoffman, J. H. Lin, G. Cuniberti, and B. Buchner, "Direct low-temperature nanographene CVD synthesis over a dielectric insulator," *Acs Nano,* vol. 4, pp. 4206-10, Jul 27 2010.

[31] G. Kalita, M. S. Kayastha, H. Uchida, K. Wakita, and M. Umeno, "Direct growth of nanographene films by surface wave plasma chemical vapor deposition and their application in photovoltaic devices," *Rsc Advances,* vol. 2, pp. 3225-3230, 2012.

[32] C. X. Marek E Schmidt1, Mike Cooke2, Hiroshi Mizuta1,3 and and H. M. H. Chong3, "Metal-free plasma-enhanced chemical vapor deposition of large area nanocrystalline graphene," *Materials Research Express 1 (2014) 025031,* 2014.

[33] R. G. Gordon, "Criteria for choosing transparent conductors," *Mrs Bulletin,* vol. 25, pp. 52-57, Aug 2000.

[34] S. De and J. N. Coleman, "Are There Fundamental Limitations on the Sheet Resistance and Transmittance of Thin Graphene Films?," *Acs Nano,* vol. 4, pp. 2713-2720, May 2010.

[35] V. C. Tung, L. M. Chen, M. J. Allen, J. K. Wassei, K. Nelson, R. B. Kaner, and Y. Yang, "Low-Temperature Solution Processing of Graphene-Carbon Nanotube Hybrid Materials for High-Performance Transparent Conductors," *Nano Lett,* vol. 9, pp. 1949-1955, May 2009.

[36] A. E. Mansour, S. Dey, A. Amassian, and M. H. Tanielian, "Bromination of Graphene: A New Route to Making High Performance Transparent Conducting Electrodes with Low Optical Losses," *ACS Appl Mater Interfaces,* vol. 7, pp. 17692-17699, Aug 19 2015.

[37] M. Aleksandrova, N. Kurtev, V. Videkov, S. Tzanova, and S. Schintke, "Material alternative to ITO for transparent conductive electrode in flexible display and photovoltaic devices," *Microelectronic Engineering,* vol. 145, pp. 112-116, Sep 1 2015.

[38] W. K. Kim, S. Lee, D. H. Lee, I. H. Park, J. S. Bae, T. W. Lee, J. Y. Kim, J. H. Park, Y. C. Cho, C. R. Cho, and S. Y. Jeong, "Cu Mesh for Flexible Transparent Conductive Electrodes," *Sci Rep,* vol. 5, Jun 3 2015.

[39] M. Song, H. J. Kim, C. S. Kim, J. H. Jeong, C. Cho, J. Y. Lee, S. H. Jin, D. G. Choi, and D. H. Kim, "ITO-free highly bendable and efficient organic solar cells with Ag nanomesh/ZnO hybrid electrodes," *Journal of Materials Chemistry A,* vol. 3, pp. 65-70, 2015.

[40] S. Chugh, R. Mehta, N. Lu, F. D. Dios, M. J. Kim, and Z. H. Chen, "Comparison of graphene growth on arbitrary non-catalytic substrates using low-temperature PECVD," *Carbon N Y,* vol. 93, pp. 393-399, Nov 2015.

[41] A. R. Barron, *Chemical Vapor Deposition*.

[42] F. J. Nelson, V. K. Kamineni, T. Zhang, E. S. Comfort, J. U. Lee, and A. C. Diebold, "Optical properties of large-area polycrystalline chemical vapor deposited graphene by spectroscopic ellipsometry," *Applied Physics Letters,* vol. 97, Dec 20 2010.

[43] S. Francilla. (2010). *Introduction-to-Micro-Fabrication (2nd ed.)*.

[44] W. Wu, Q. K. Yu, P. Peng, Z. H. Liu, J. M. Bao, and S. S. Pei, "Control of thickness uniformity and grain size in graphene films for transparent conductive electrodes," *Nanotechnology,* vol. 23, Jan 27 2012.

[45] R. Saito, M. Hofmann, G. Dresselhaus, A. Jorio, and M. S. Dresselhaus, "Raman spectroscopy of graphene and carbon nanotubes," *Advances in Physics,* vol. 60, pp. 413-550, 2011.

[46] G. Fisichella, S. Di Franco, P. Fiorenza, R. Lo Nigro, F. Roccaforte, C. Tudisco, G. G. Condorelli, N. Piluso, N. Sparta, S. Lo Verso, C. Accardi, C. Tringali, S. Ravesi, and F. Giannazzo, "Micro- and nanoscale electrical characterization of large-area graphene transferred to functional substrates," *Beilstein J Nanotechnol,* vol. 4, pp. 234-42, 2013.

[47] Chang-Soo Park,[*a] Yu Zhao,[a] Heetae Kim,[b] Yoon Shon[c] and Eun Kyu Kim[d], "Resistivity peaks and magnetic properties of an annealed graphene," *Chem. Commun.,* 2014, 50, 12930.